

0 200 400 600 800 1000m

Fig. II-2-35 IP plane map of n=3 in Maqail area

A

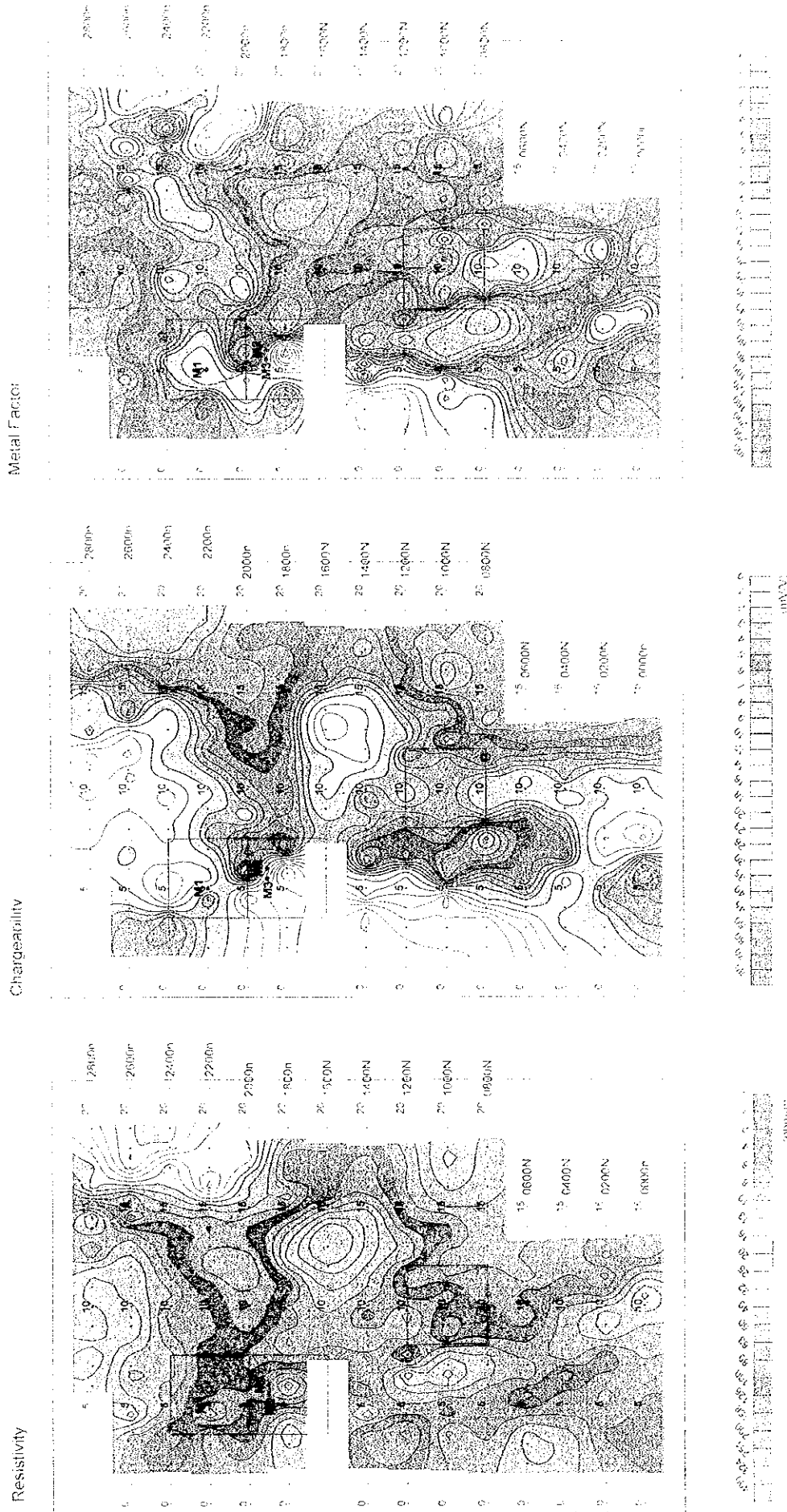


Fig. II-2-35 IP plane map of n-3 in Maqail area

Figure 11

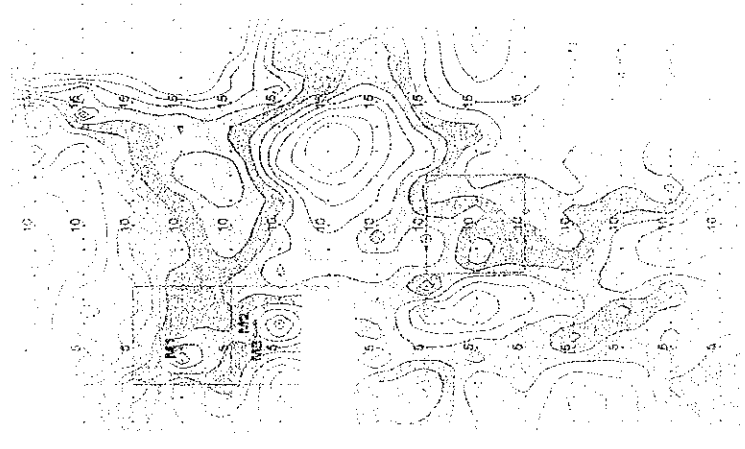


Figure 12

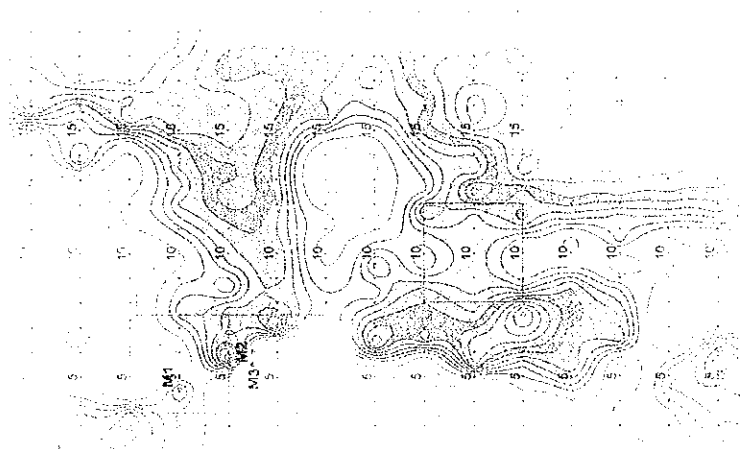
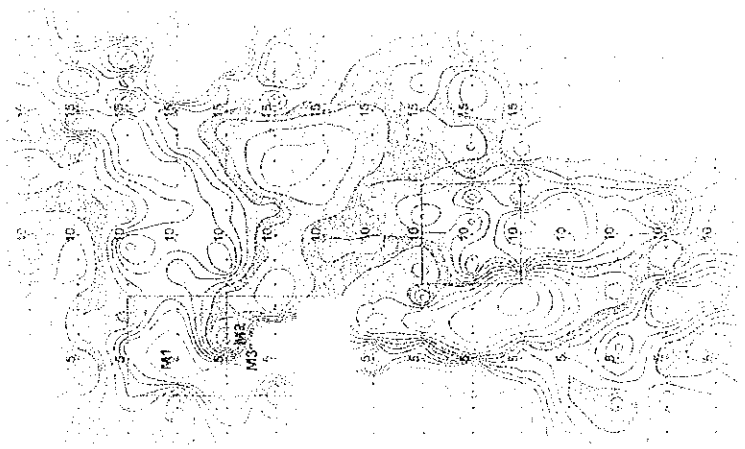
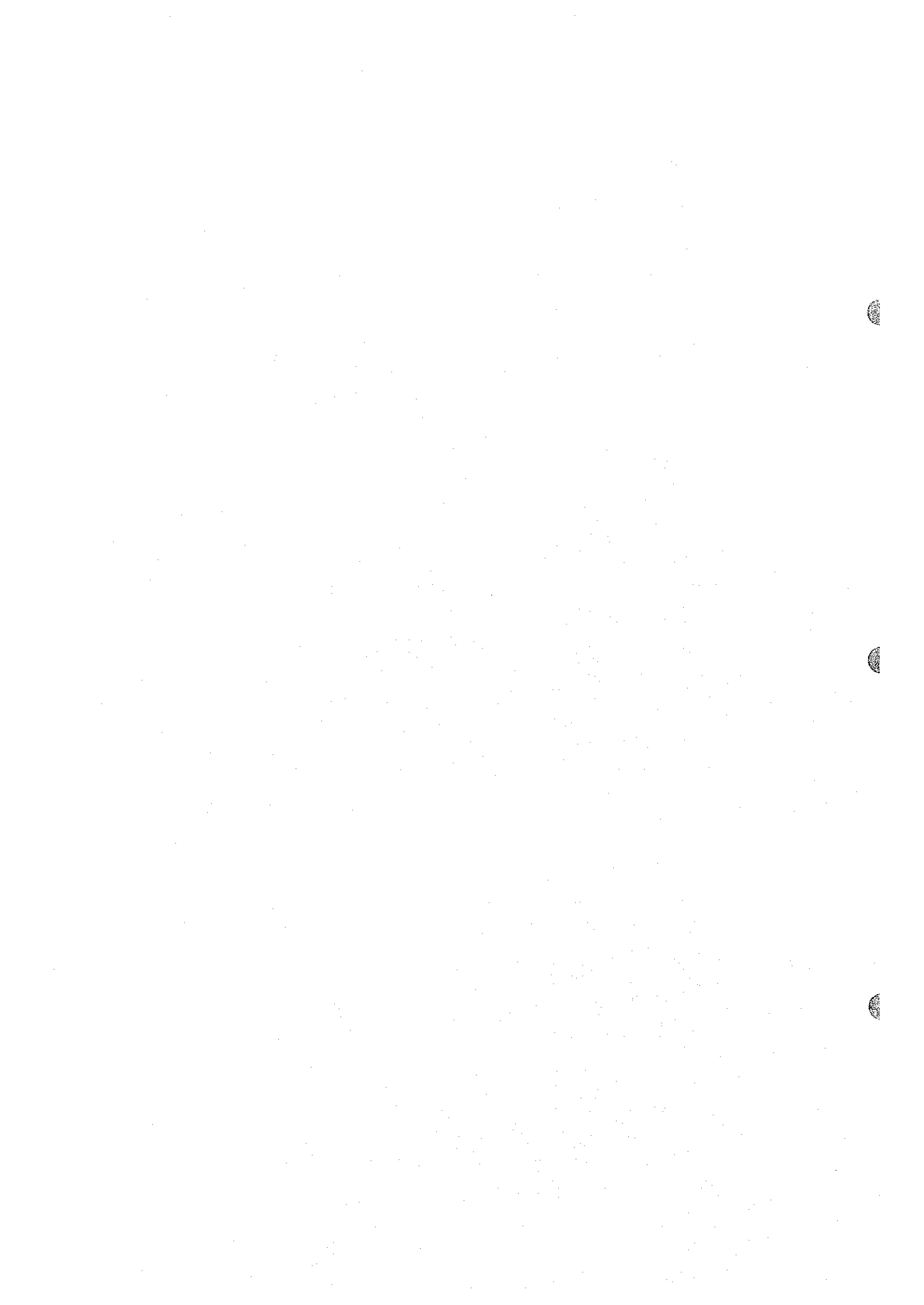


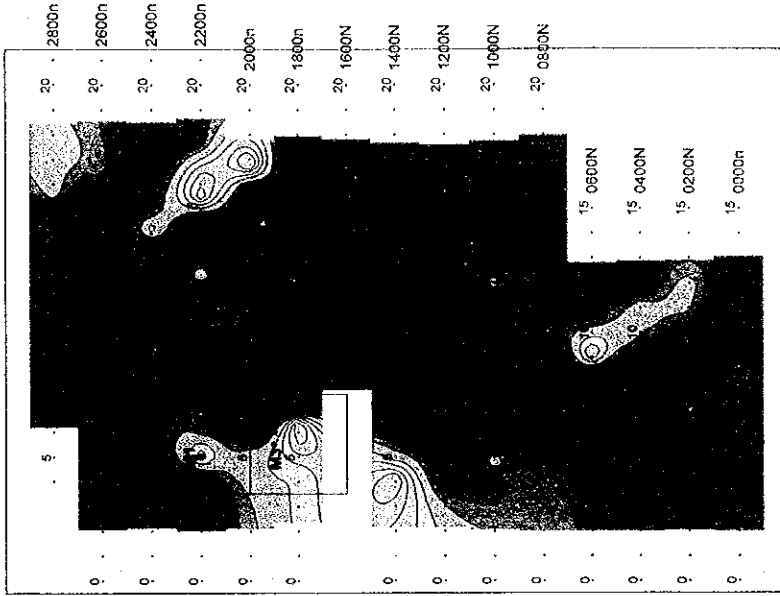
Figure 13



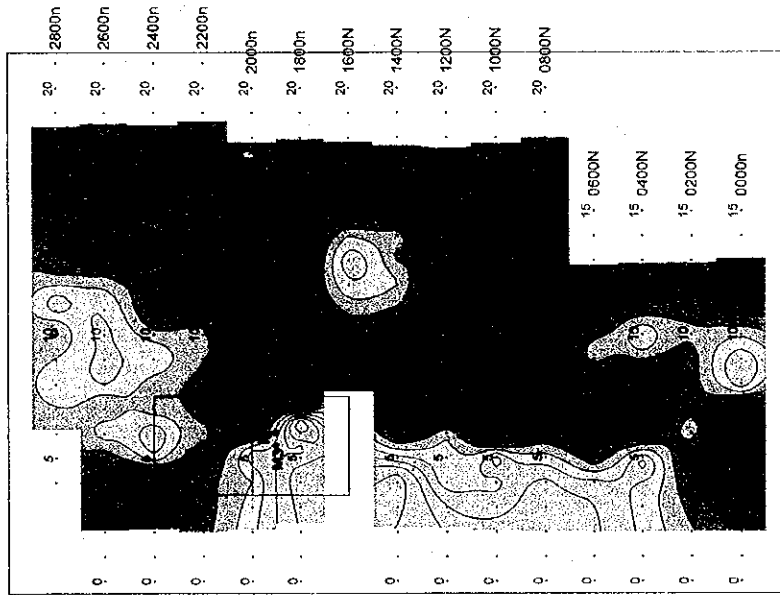




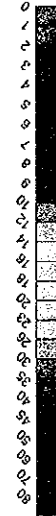
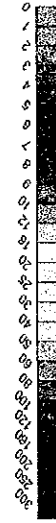
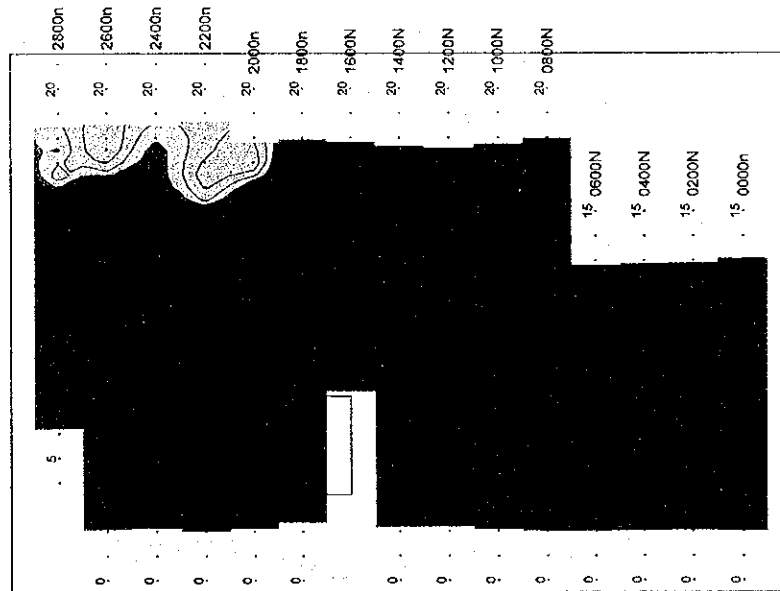
Metal Factor



Chargeability



Resistivity



- : Borehole
- : TEM Survey area

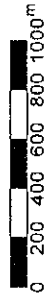


Fig. II -2-36 IP plane map of n=4 in Maqail area

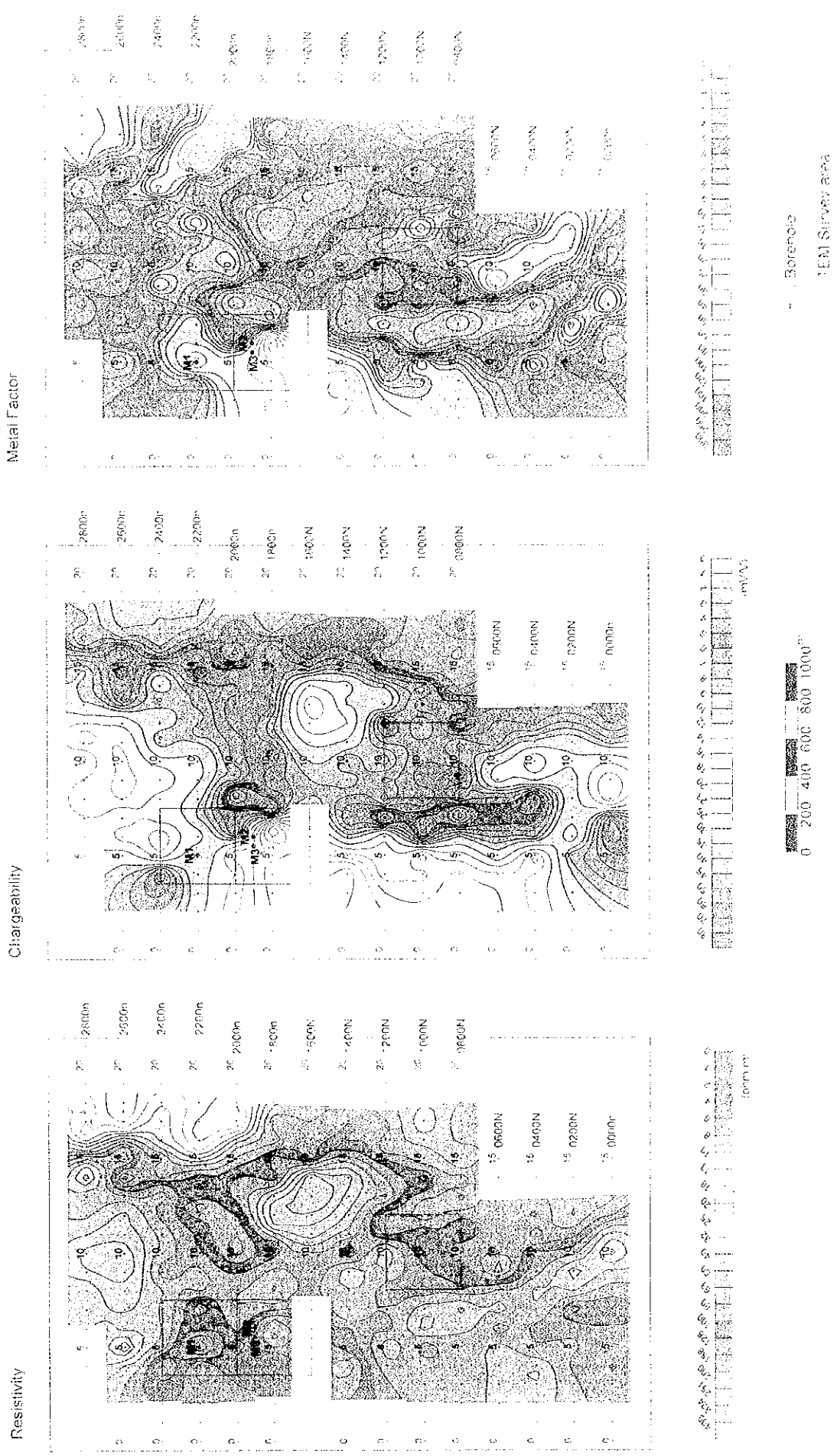


Fig. II-2-5c IP plane map of a-4 in Maqali area

Figure 10

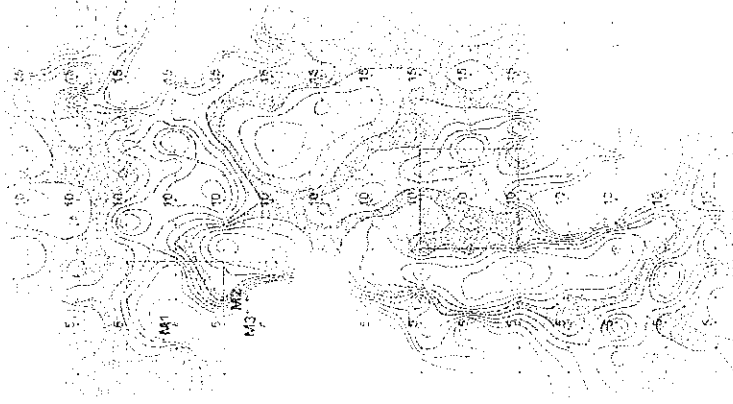


Figure 11



Figure 12

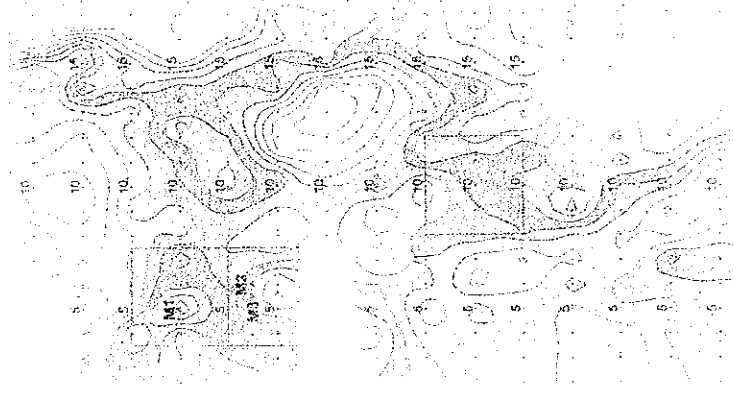
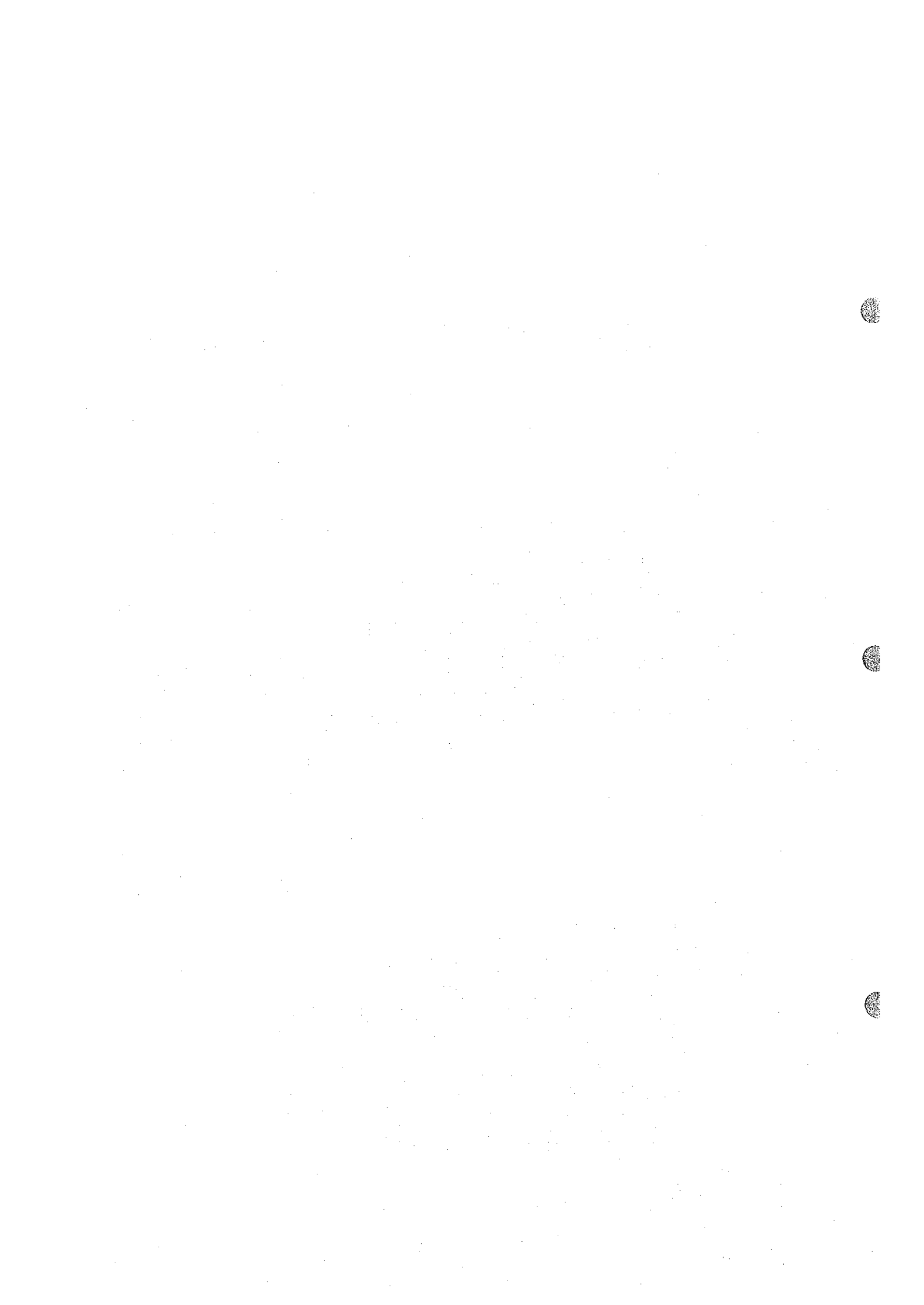


Figure 10  
Figure 11  
Figure 12

Figure 10  
Figure 11  
Figure 12

Figure 10  
Figure 11  
Figure 12





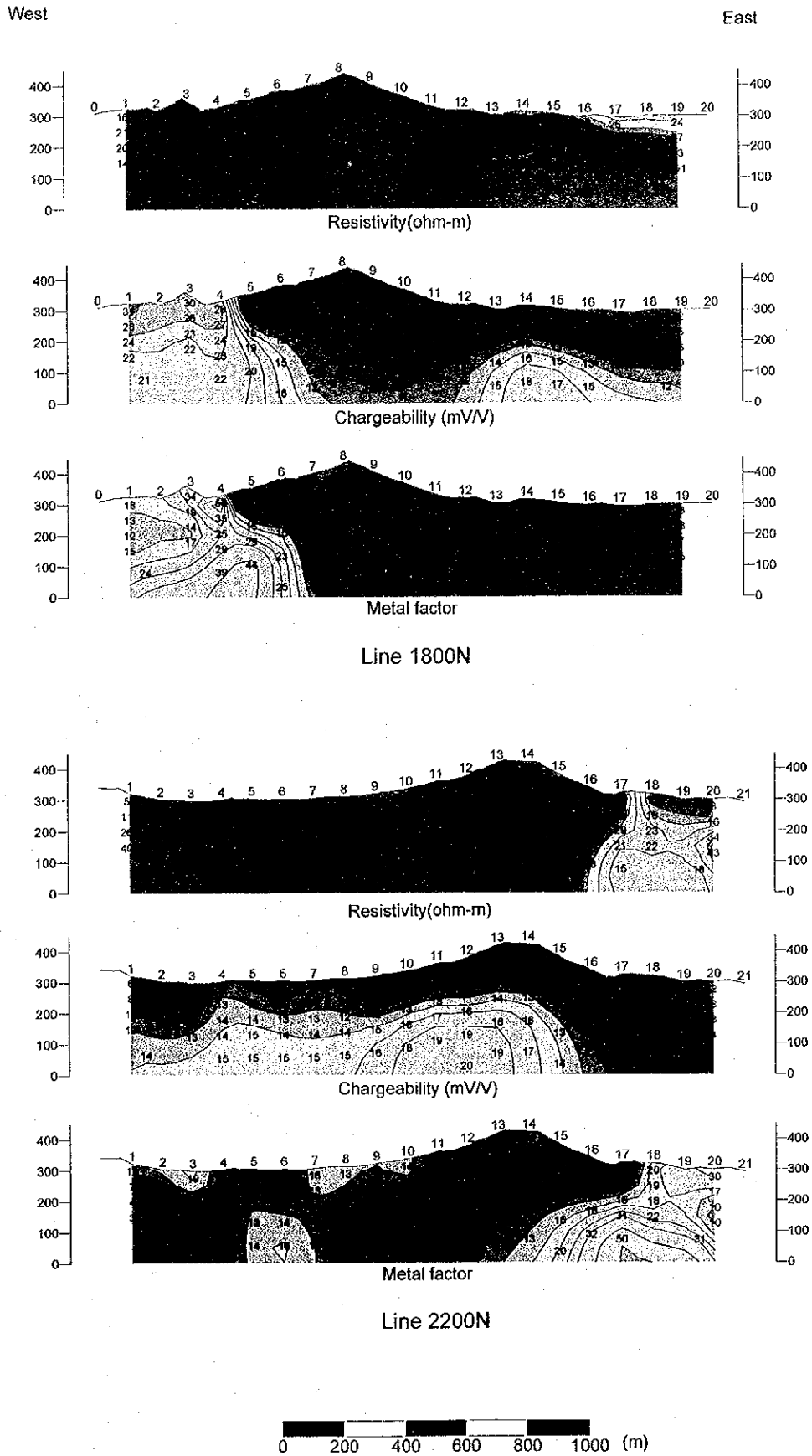
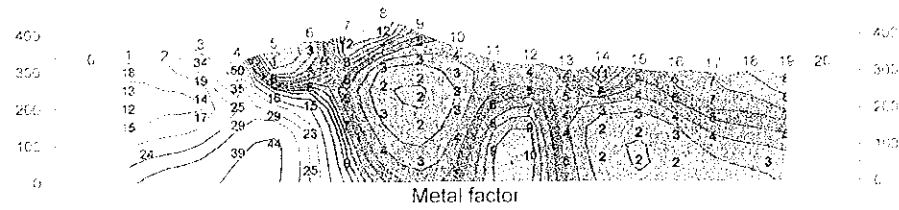
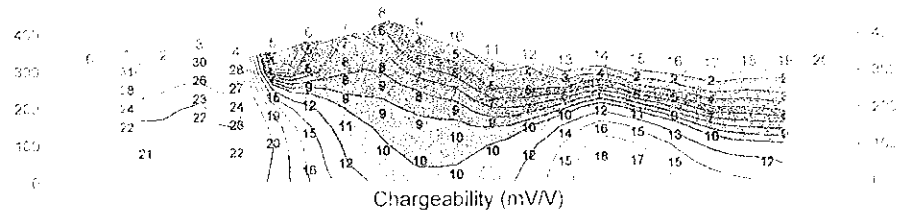
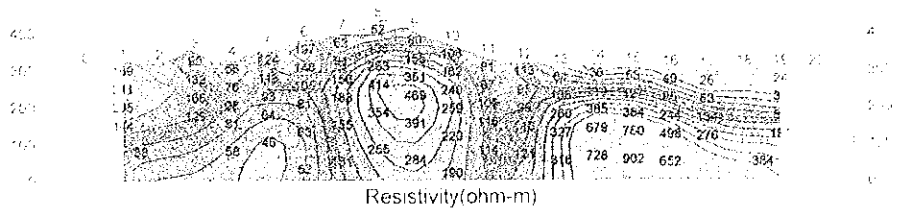


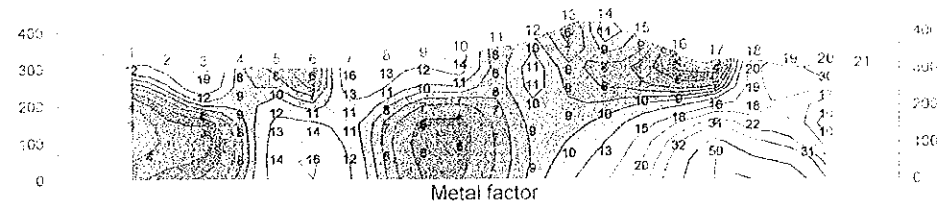
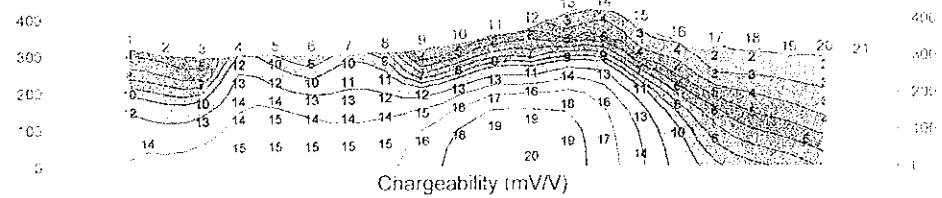
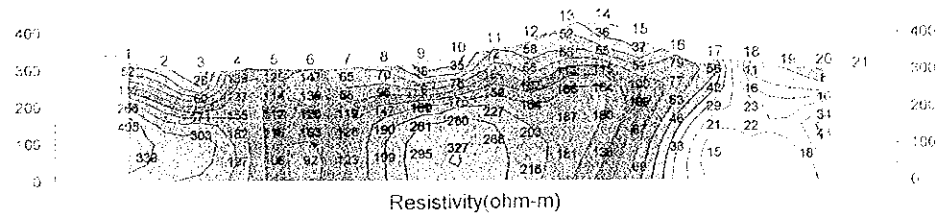
Fig. II -2-37 IP 2D model simulation on lines 1800N and 2200N in Maqail area

West

East



Line 1800N



Line 2200N



Fig. II -2-37 IP 2D model simulation on lines 1800N and 2200N in Maqail area

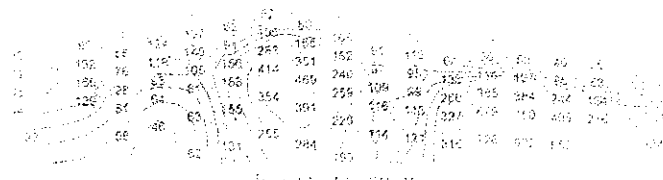


Figure 21.1.1



Figure 21.1.2

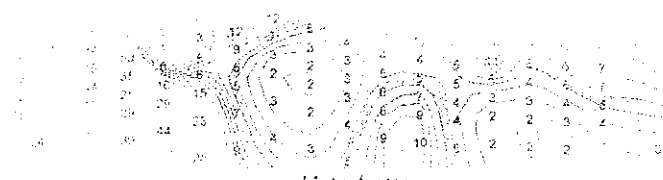


Figure 21.1.3

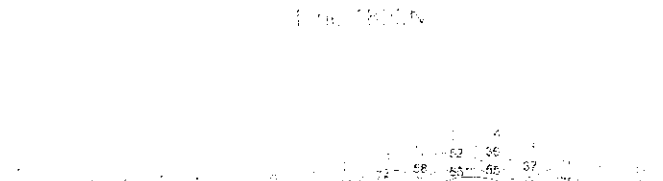


Figure 21.1.4

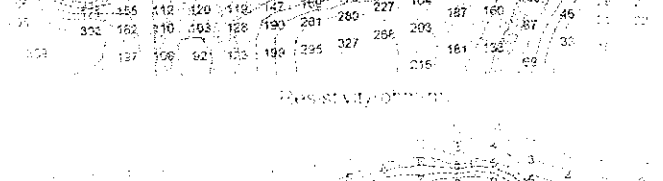


Figure 21.1.5

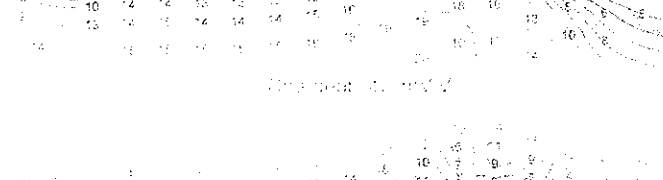


Figure 21.1.6

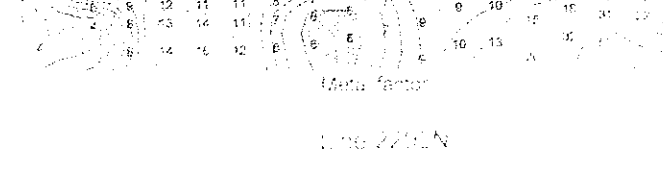


Figure 21.1.7

Figure 21.1.8

Figure 21.1.9



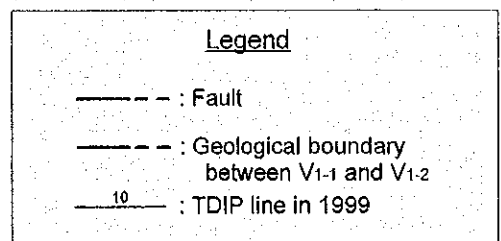
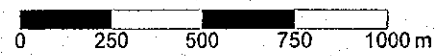
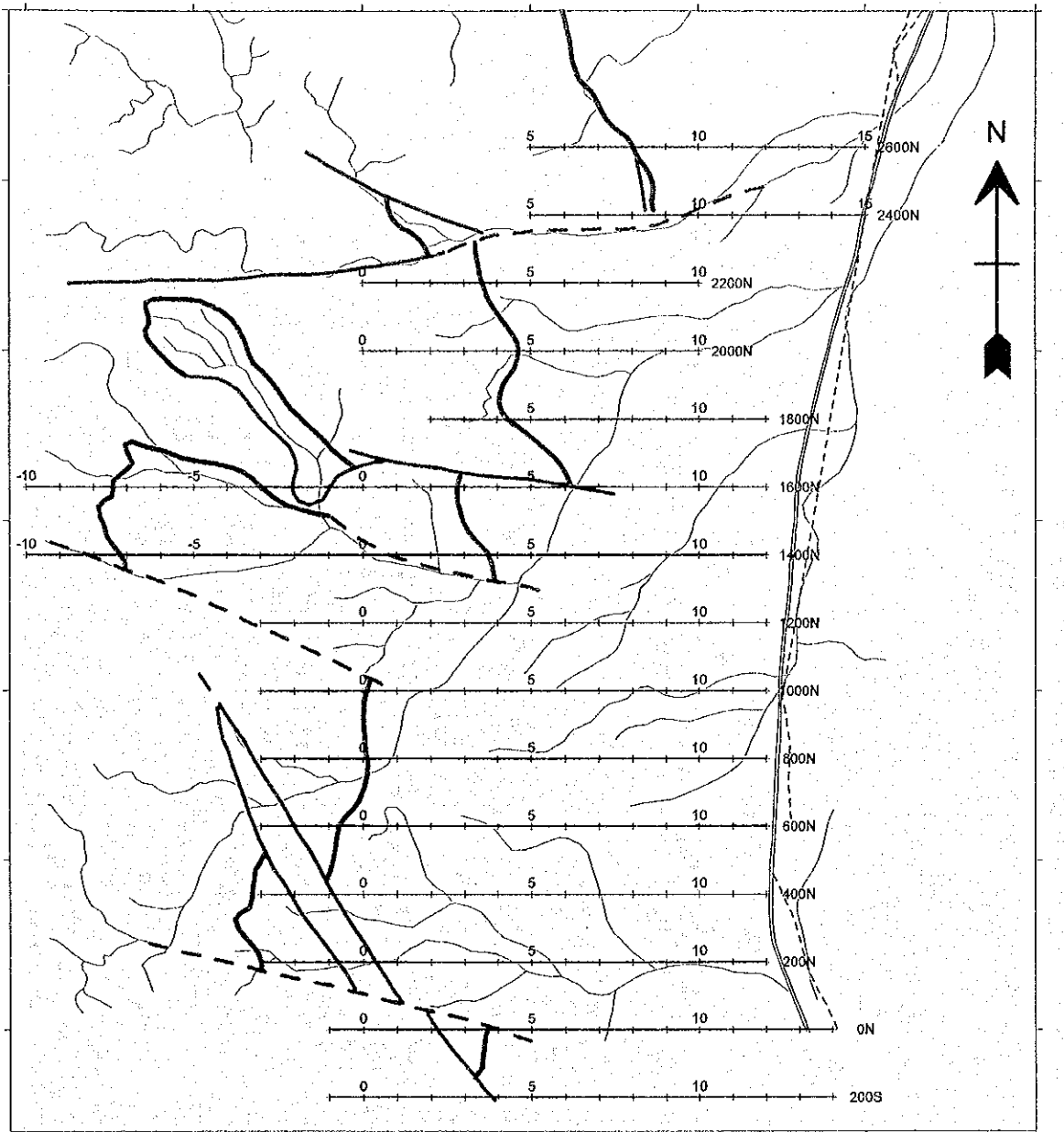


Fig. II -2-38 Geophysical survey location in Salahi area



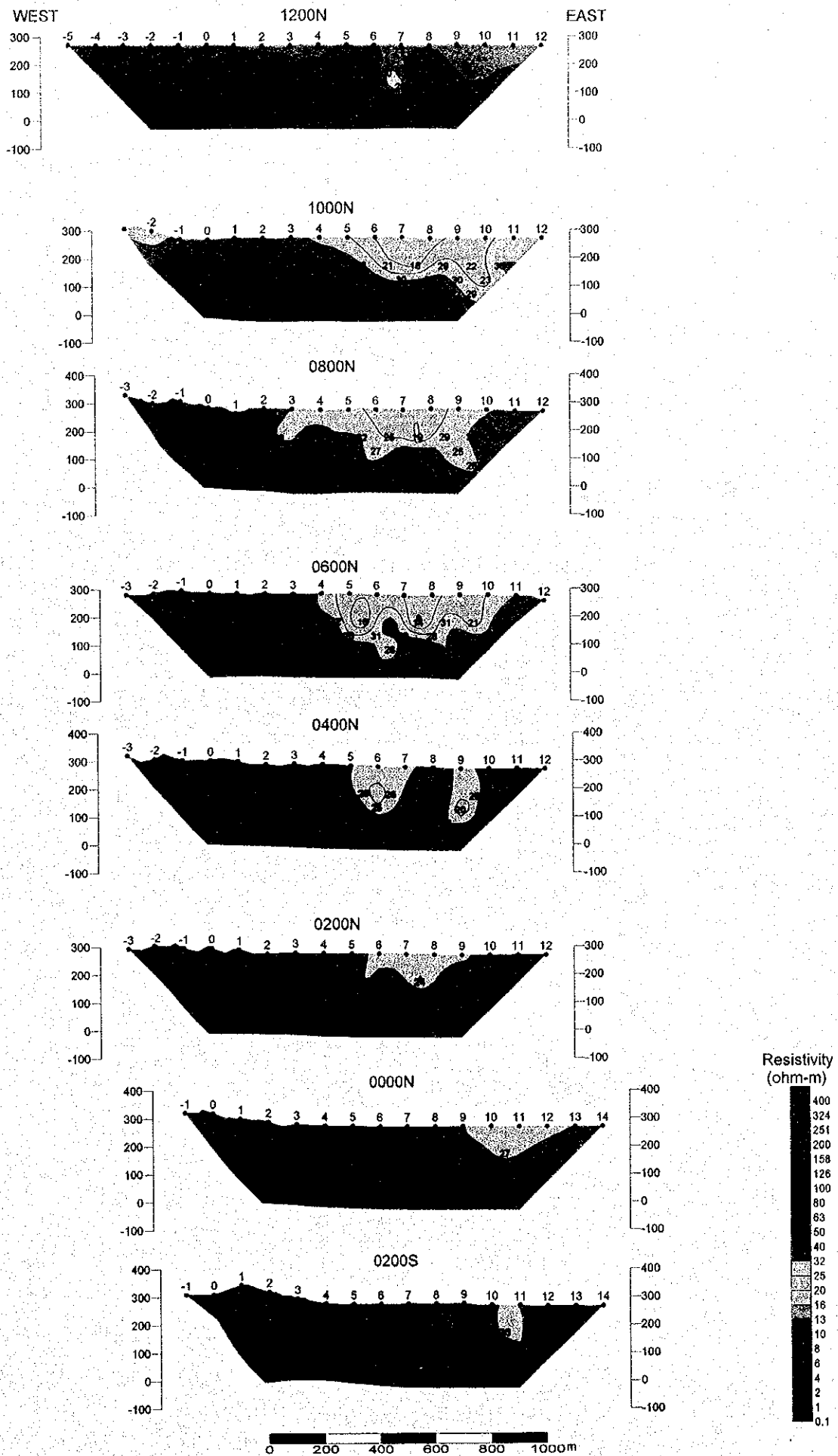


Fig. II-2-39(1) Apparent resistivity pseudo-sections in Salahi area

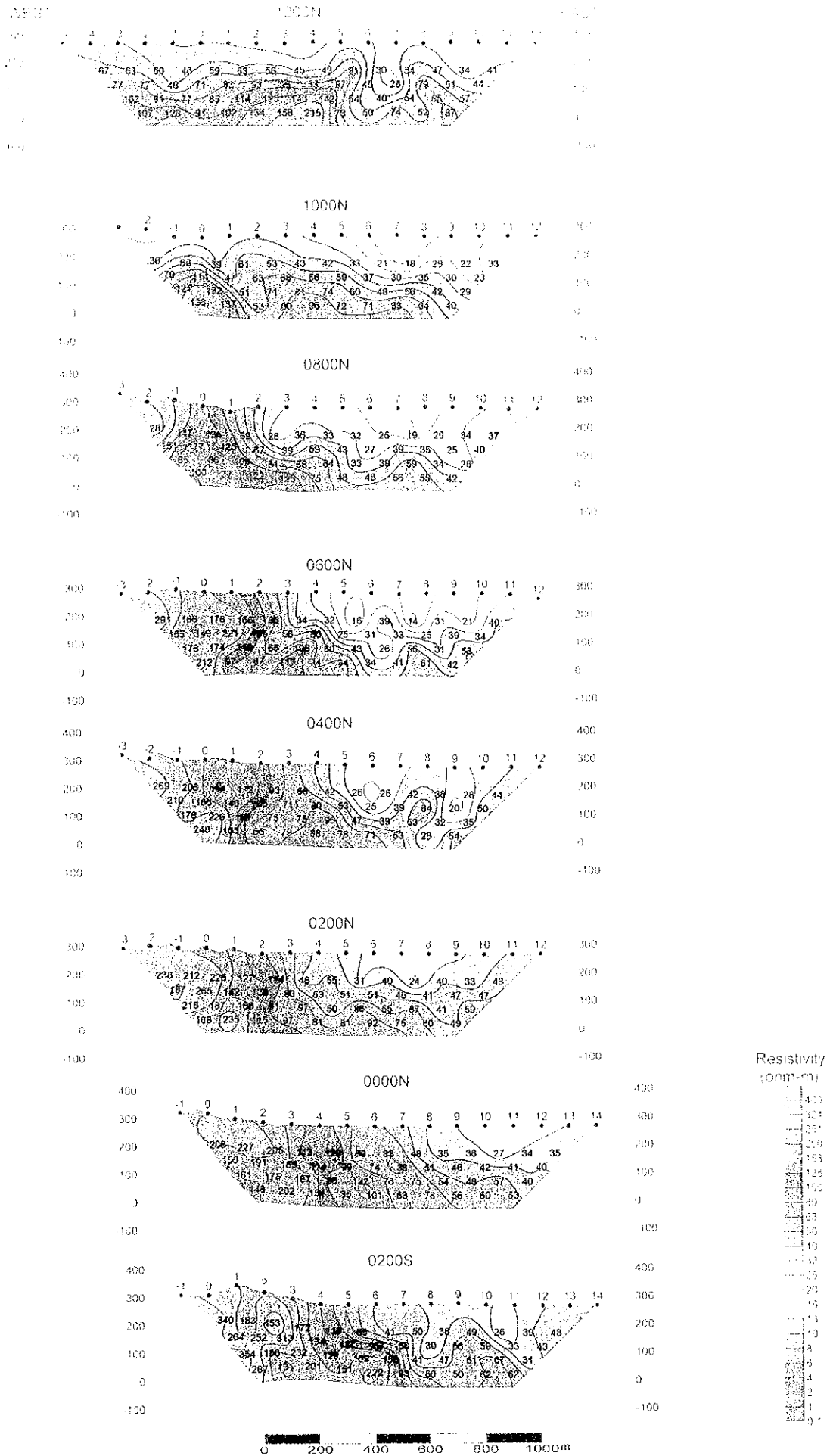


Fig. II-2-39(1) Apparent resistivity pseudo-sections in Salahi area



43 50 45 52 33 58 45 49 41 37 34 47 34  
 37 37 48 41 48 50 50 50 50 50 50 50 50  
 21 31 27 35 14 105 130 140 150 40 54 25 22  
 107 108 101 102 114 153 114 79 59 57 57 57

39 100 39 81 53 43 42 34 27 18 23 22 21  
 114 47 83 68 26 39 37 30 35 33 31  
 121 130 51 71 61 74 60 48 58 42 37  
 135 131 53 30 56 72 75 83 34 36

147 135 64 24 36 33 31 21 19 29 34 31  
 107 77 126 67 39 53 43 27 35 35 30 40  
 85 69 109 61 26 34 33 39 53 34 26  
 100 77 122 25 75 48 46 58 33 42

169 175 168 85 24 33 19 39 44 31 21 48  
 155 149 221 105 56 20 25 31 33 75 39 34  
 176 174 149 65 88 80 43 28 55 31 52  
 212 97 87 47 74 94 34 41 51 42

208 184 172 83 60 42 26 26 42 36 24 44  
 219 168 149 105 71 60 33 25 35 54 20 53  
 175 226 60 75 75 95 47 39 53 32 35  
 248 133 66 75 68 78 71 33 23 54

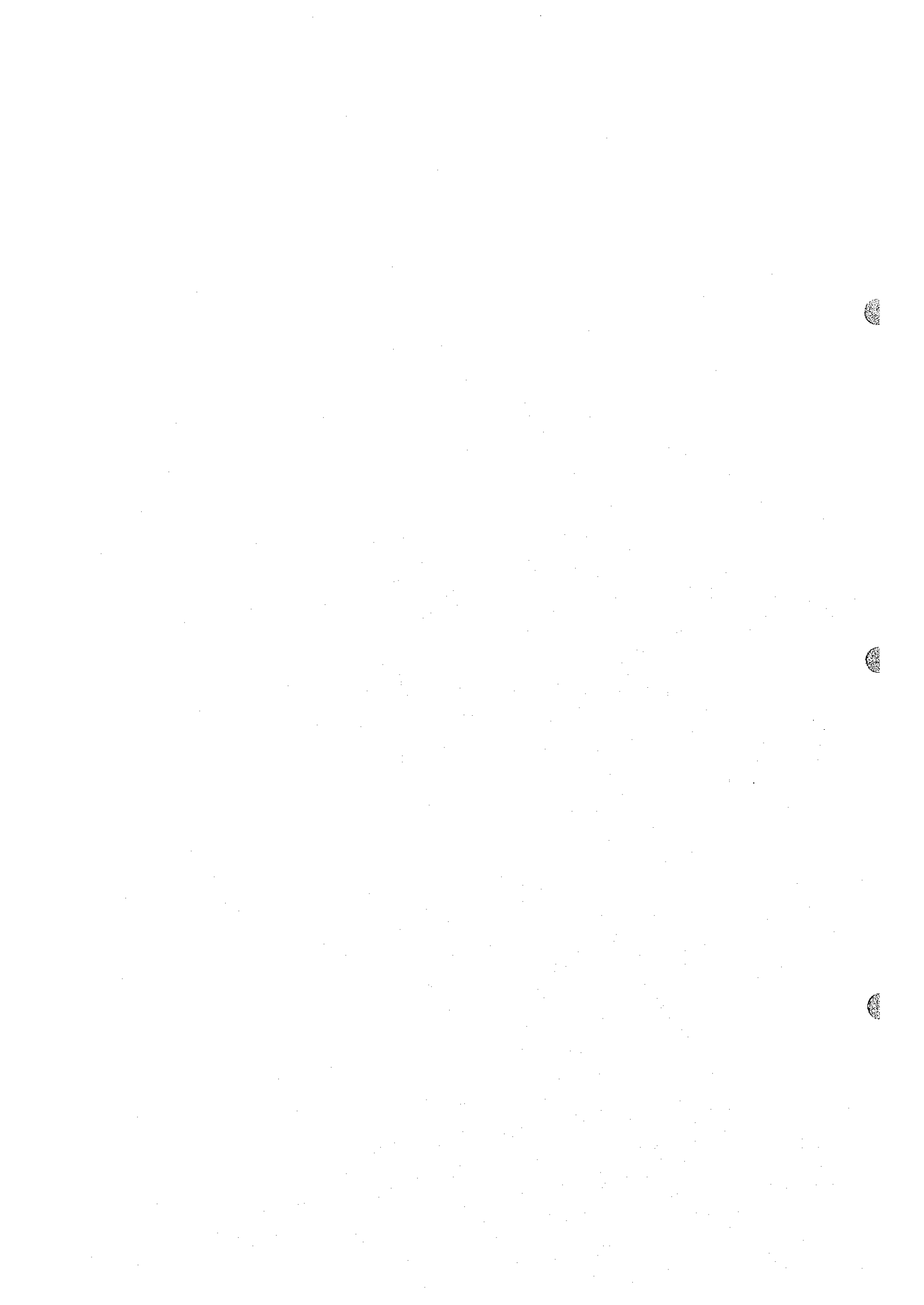
212 228 127 116 46 53 31 40 24 40 33 49  
 187 265 142 138 40 53 51 51 45 41 47 47  
 210 187 168 41 97 50 85 55 67 41 59  
 195 233 145 87 31 31 92 75 50 49

227 205 113 128 50 83 48 35 26 27 34 35  
 155 191 165 114 69 74 33 31 46 42 41 40  
 181 175 181 88 102 76 75 54 48 57 40  
 148 202 134 35 101 69 76 56 60 50

183 153 172 118 65 41 50 39 49 26 38 48  
 264 252 312 134 127 107 89 30 56 59 33 43  
 254 186 232 128 163 158 41 47 61 37 31  
 267 131 201 191 222 89 69 50 62 62

APPENDIX APPENDIX APPENDIX

Appendixes (Part 1) - Appendixes (Part 2) - Appendixes (Part 3)



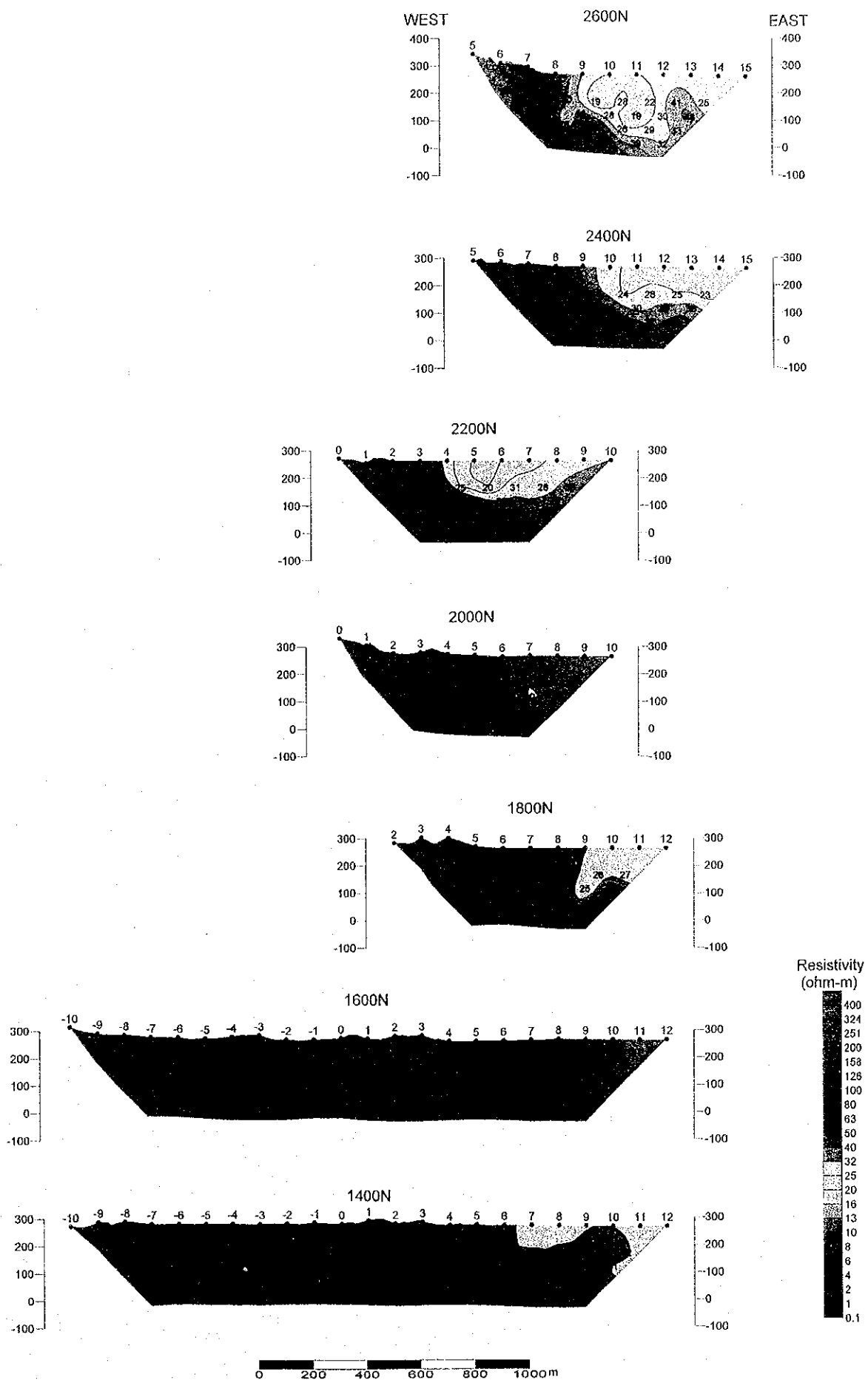


Fig. II-2-39(2) Apparent resistivity pseudo-sections in Salahi area

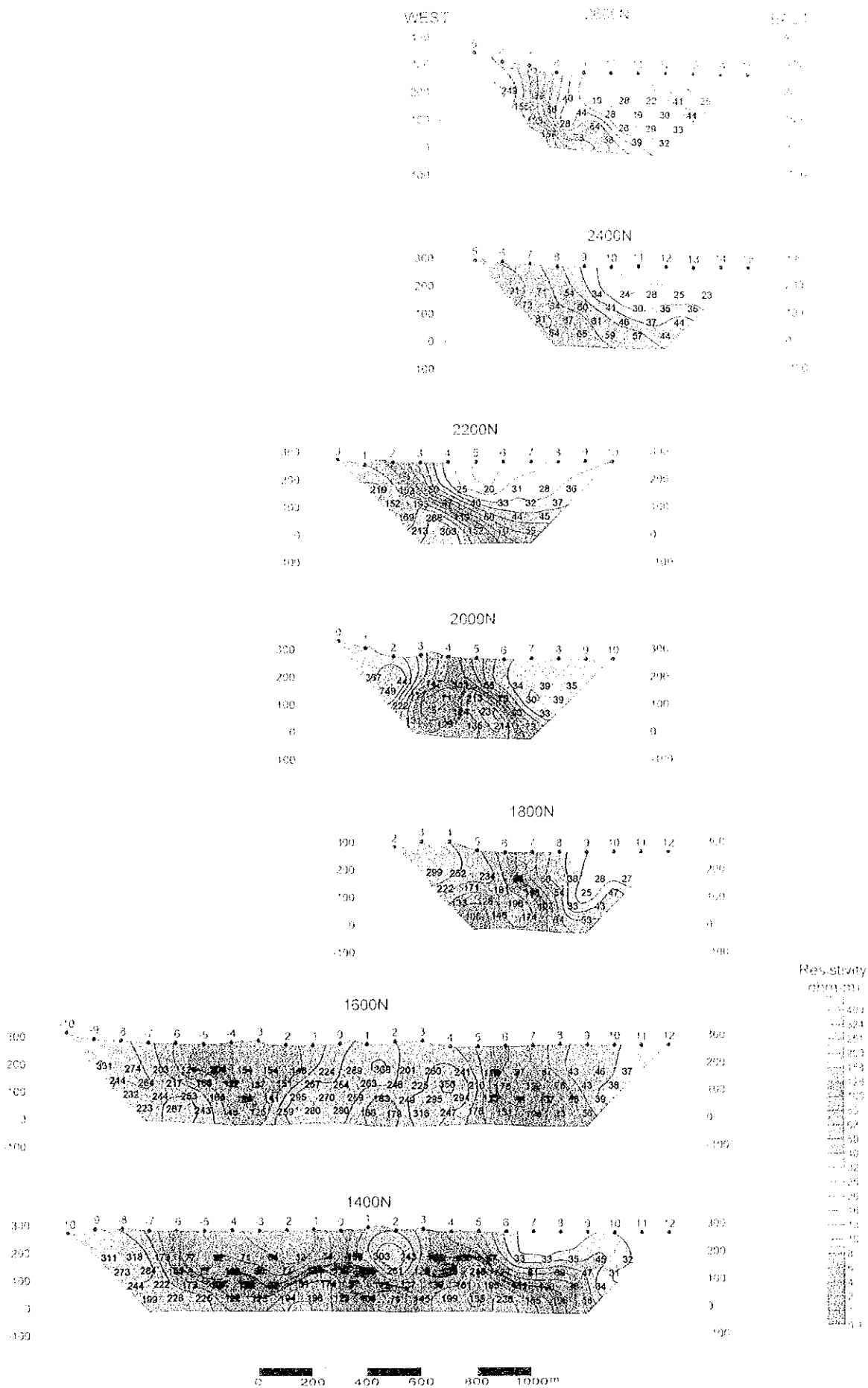


Fig. II -2-39(2) Apparent resistivity pseudo-sections in Sahi area





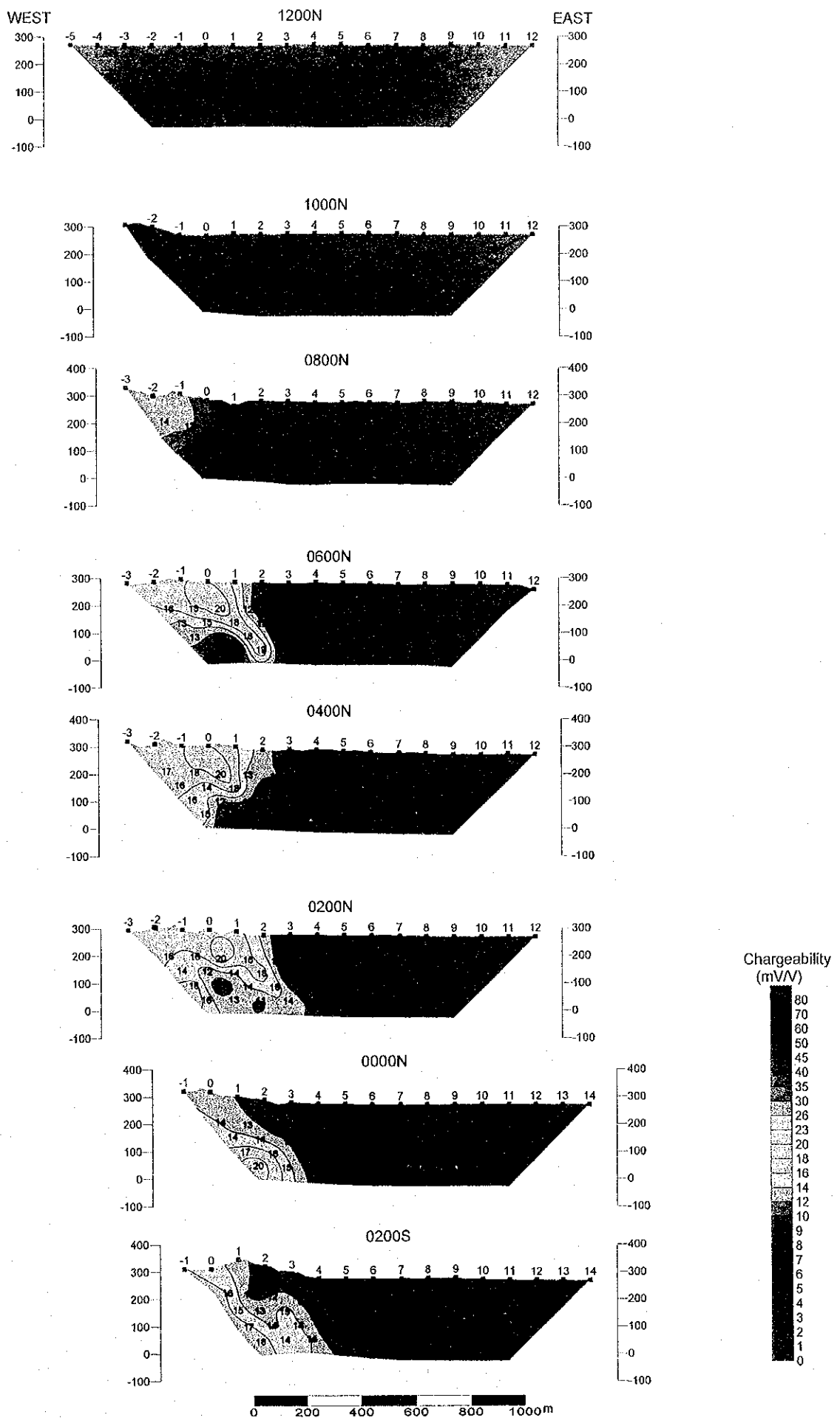


Fig. II-2-40(1) Chargeability pseudo-sections in Salahi area

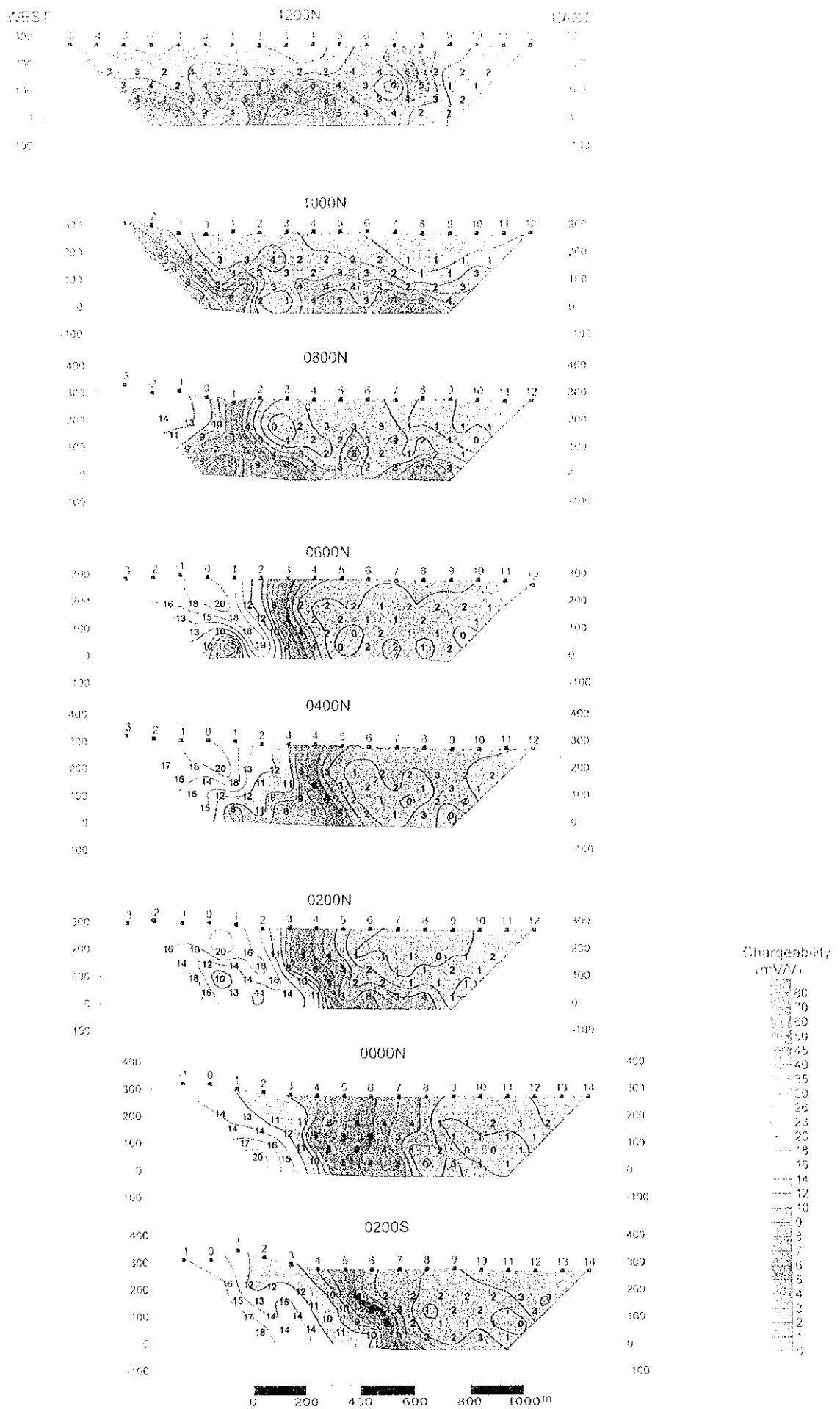


Fig. II -2-40(1) Chargeability pseudo-sections in Salahi area



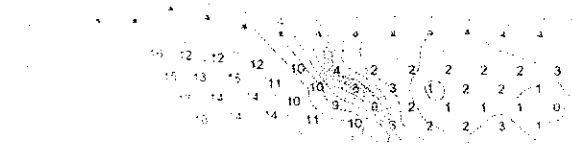
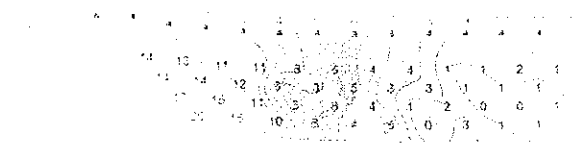
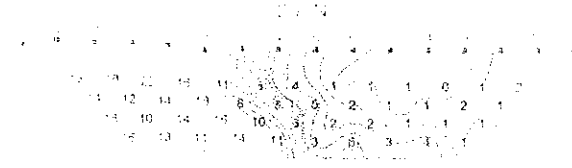
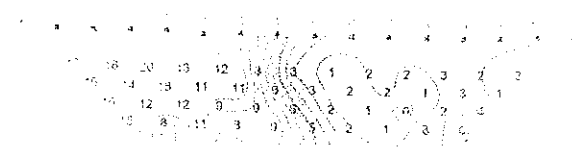
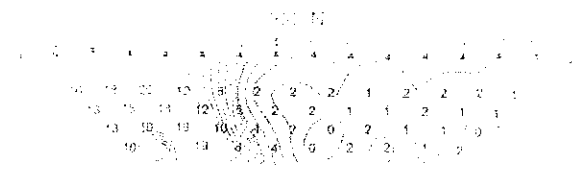
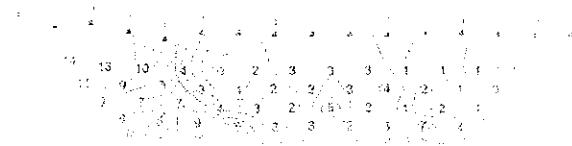
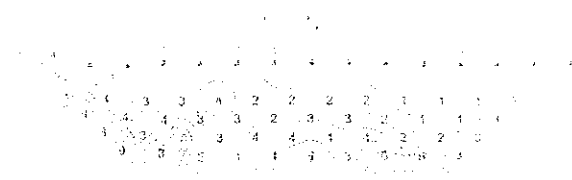
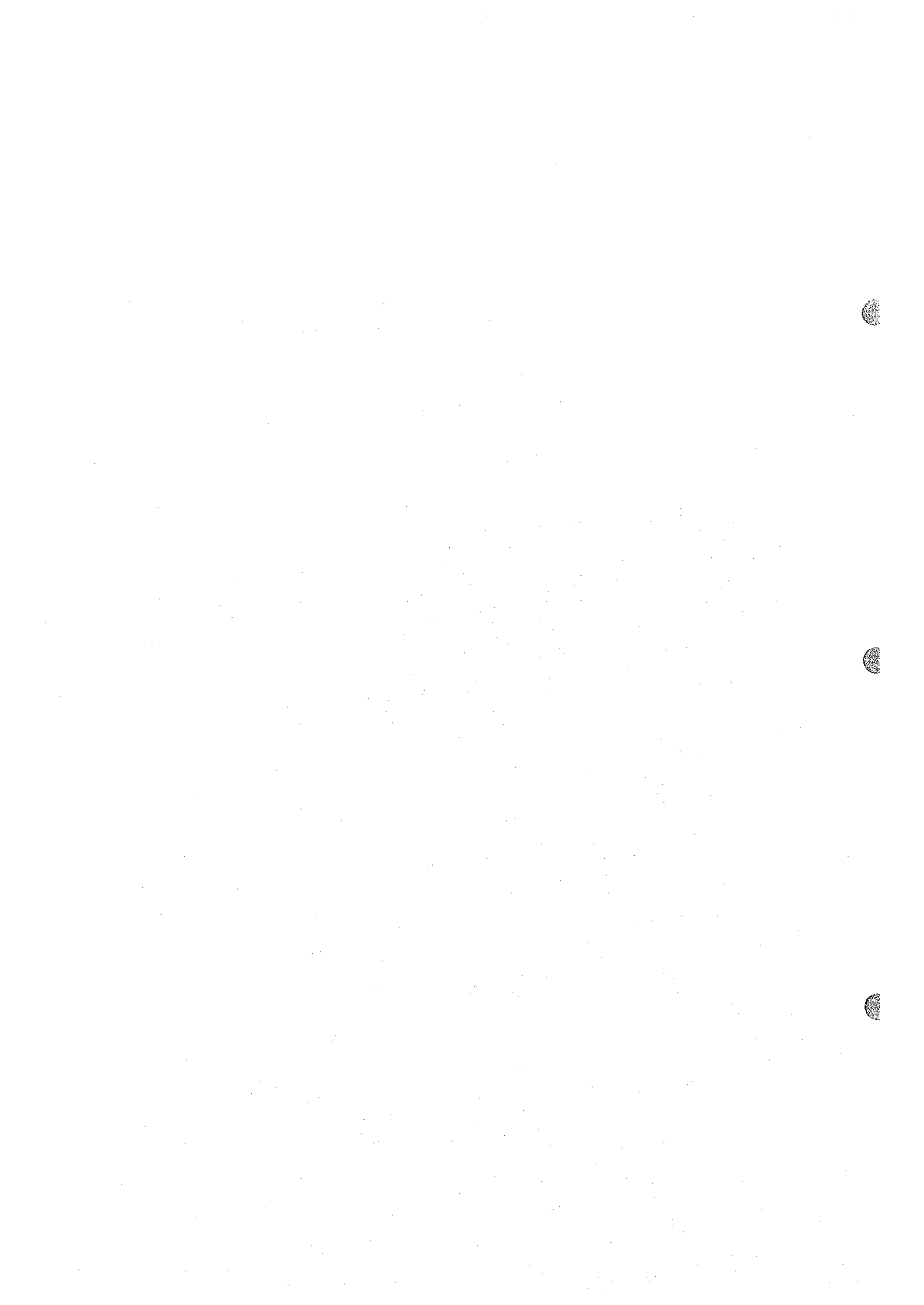


Figure 1: Contour plot of the distribution of the variable  $X$  for the parameter values  $\theta = 1$ . The plot shows a central peak with several smaller peaks and valleys. The axes are labeled with numerical values, and the contours are represented by dashed lines.

Figure 1-8: Contour plots of the distribution of the variable  $X$  for the parameter values  $\theta = 1, 2, 3, 4, 5, 6, 7, 8$ .



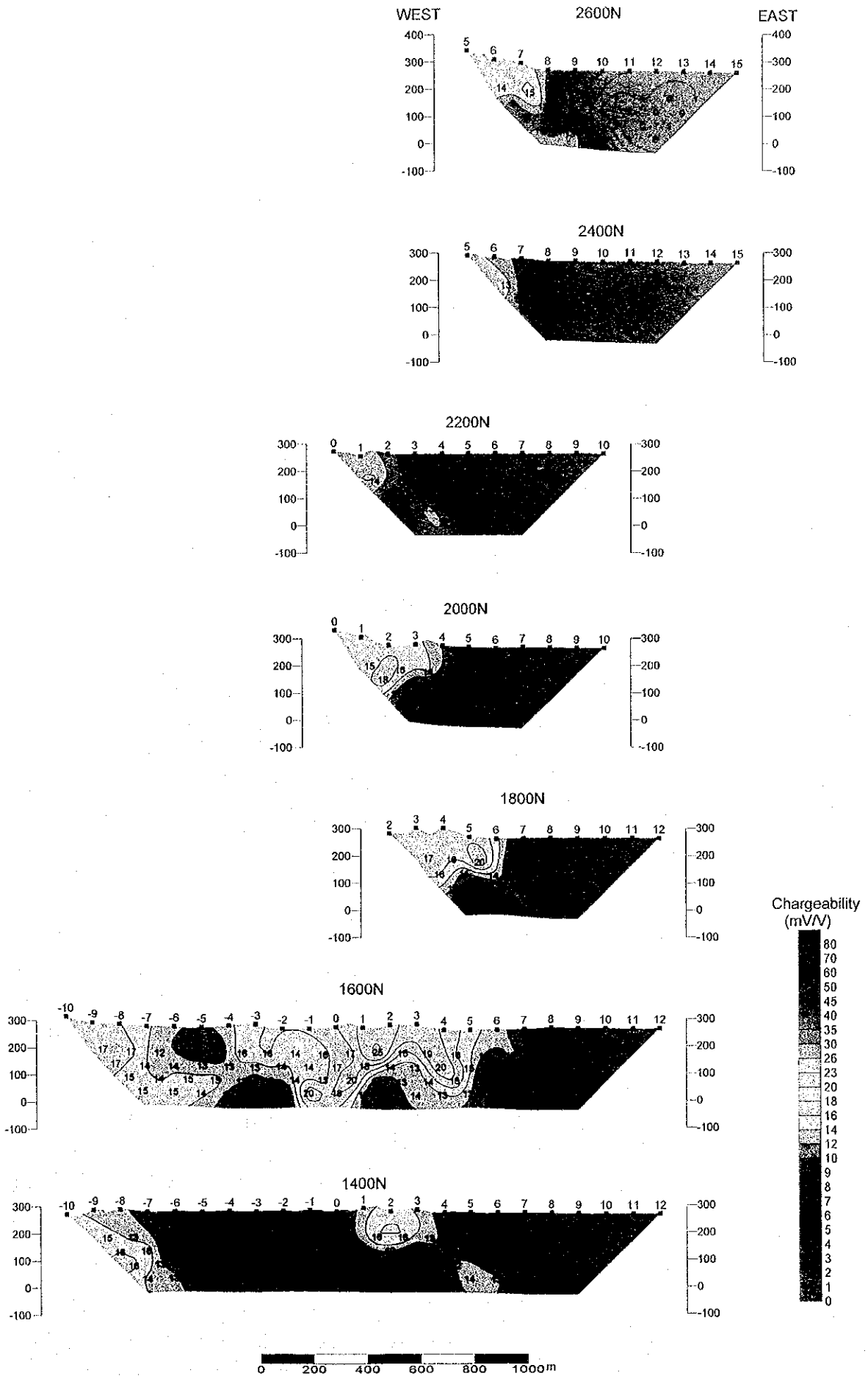


Fig. II -2-40(2) Chargeability pseudo-sections in Salahi area

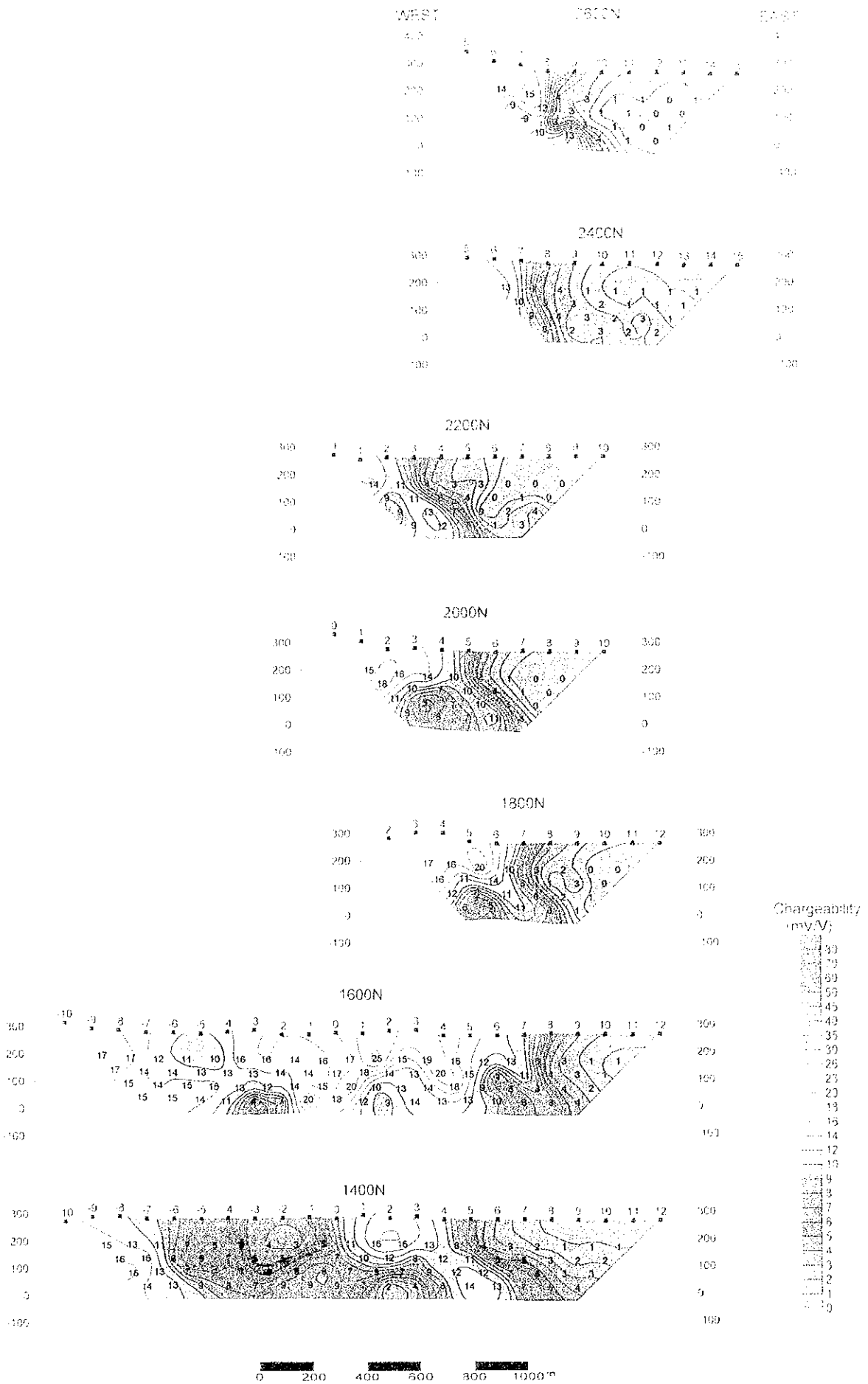


Fig. II -2-40(2) Chargeability pseudo-sections in Salahi area

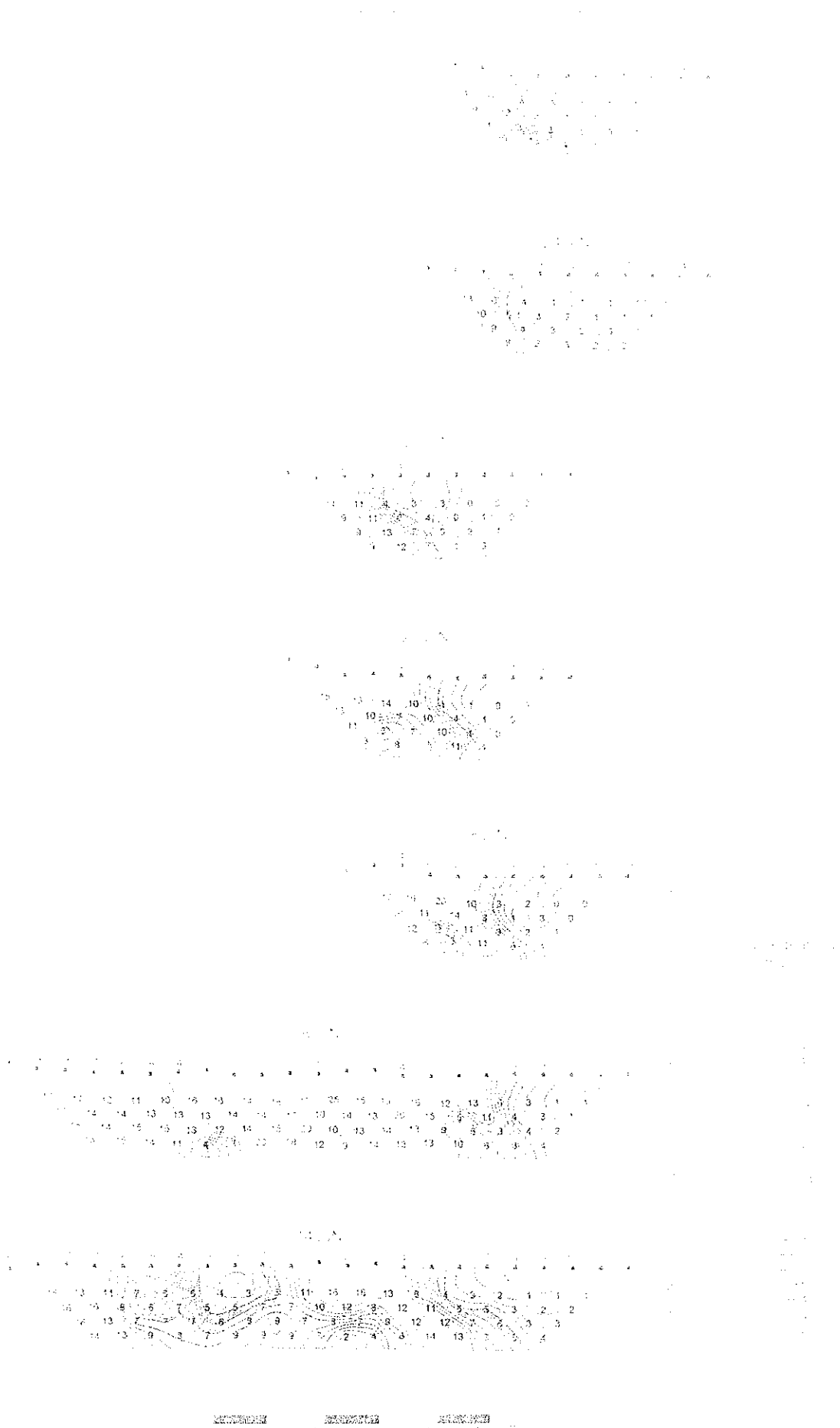
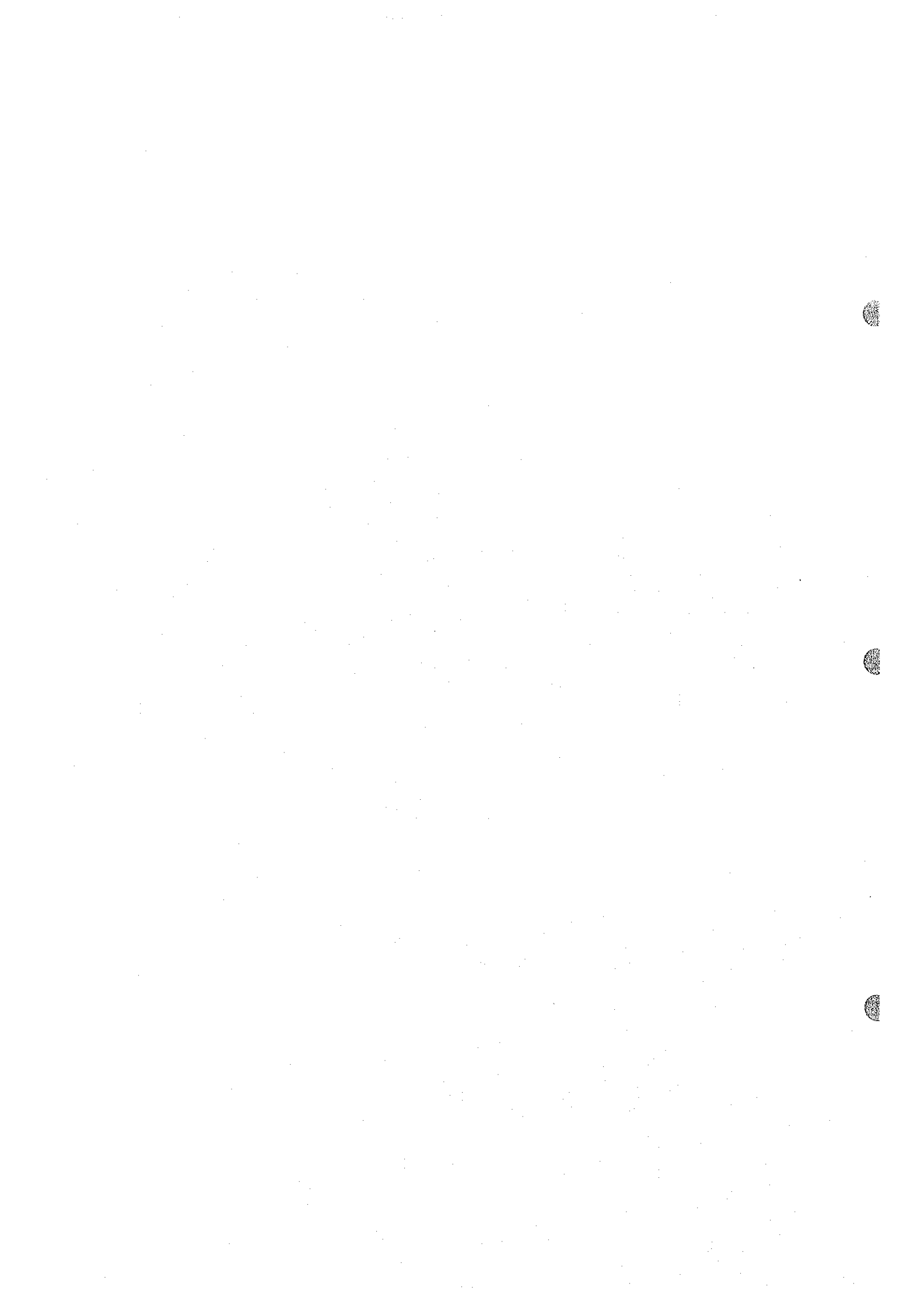


图 11-2-4-2 浅海探测概率分布图



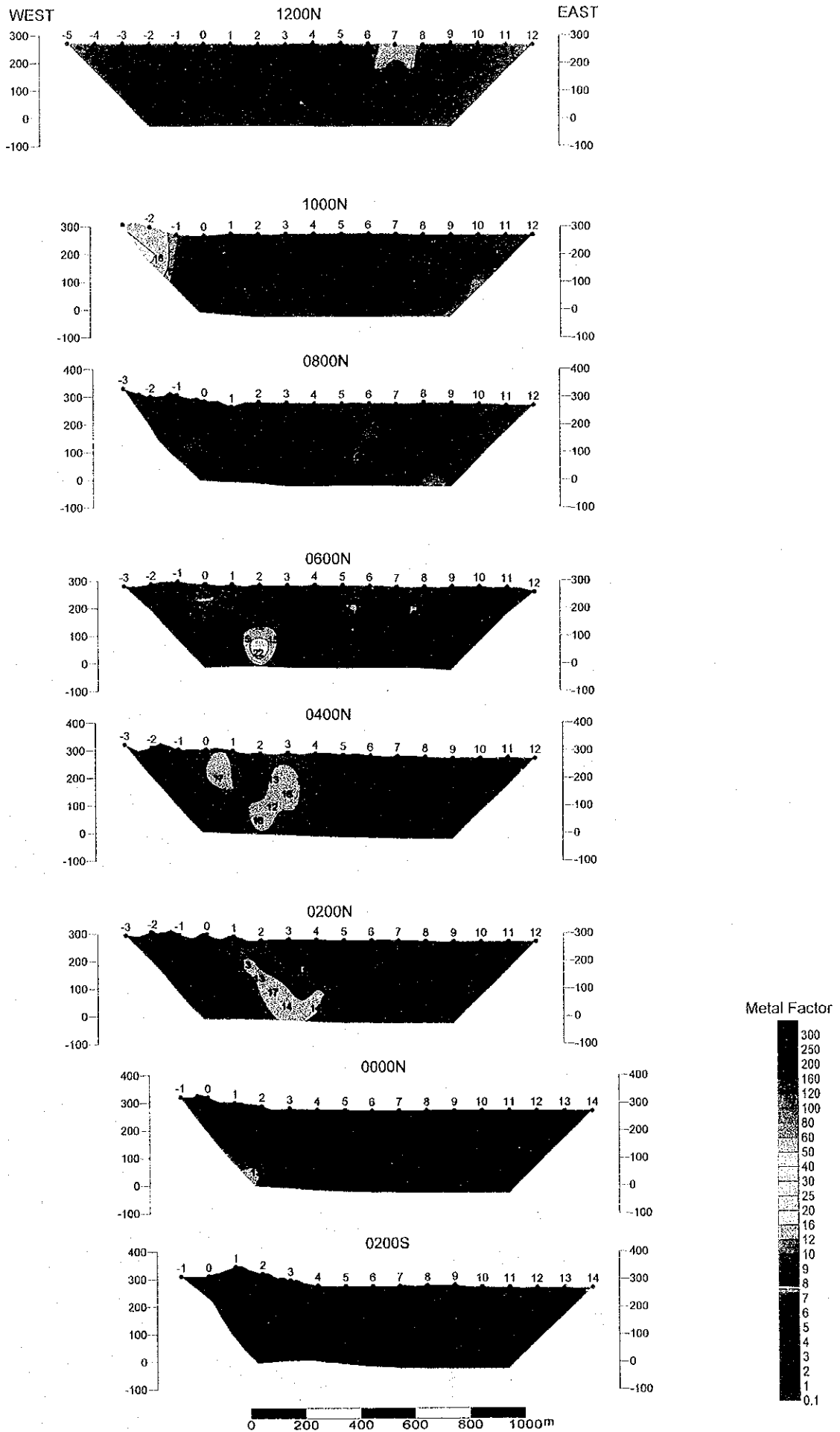


Fig. II-2-41(1) Metal factor pseudo-sections in Salahi area

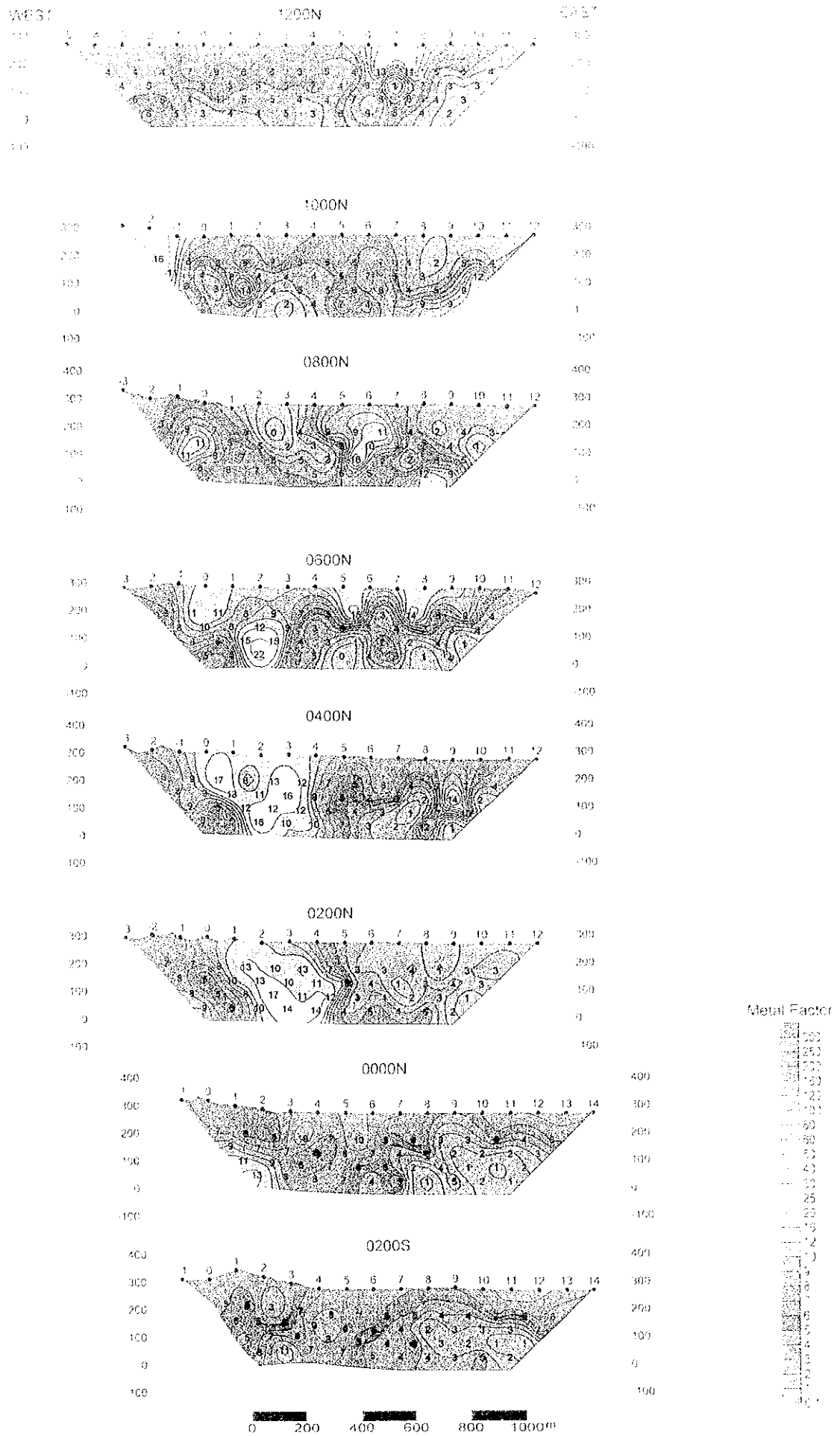


Fig. II -2-41(1) Metal factor pseudo-sections in Salahi area



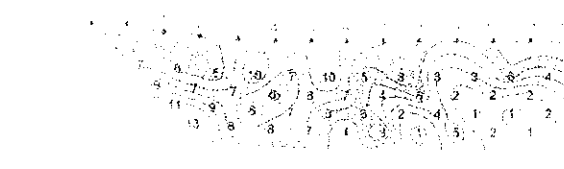
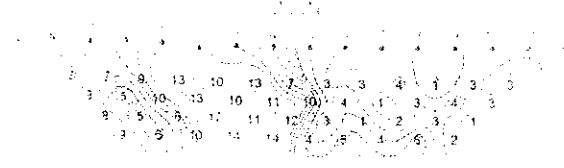
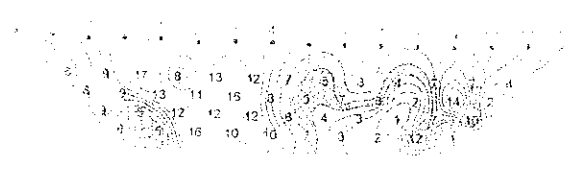
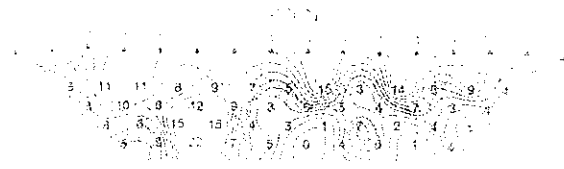
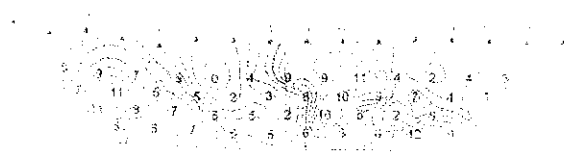
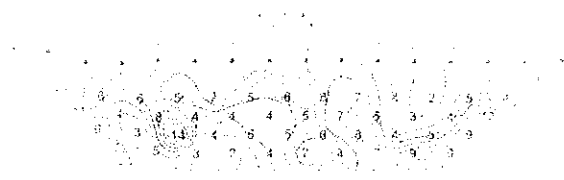


Figure 10.10: Manufacturing cost function in 2D

Fig. 10.10: Manufacturing cost function in 2D



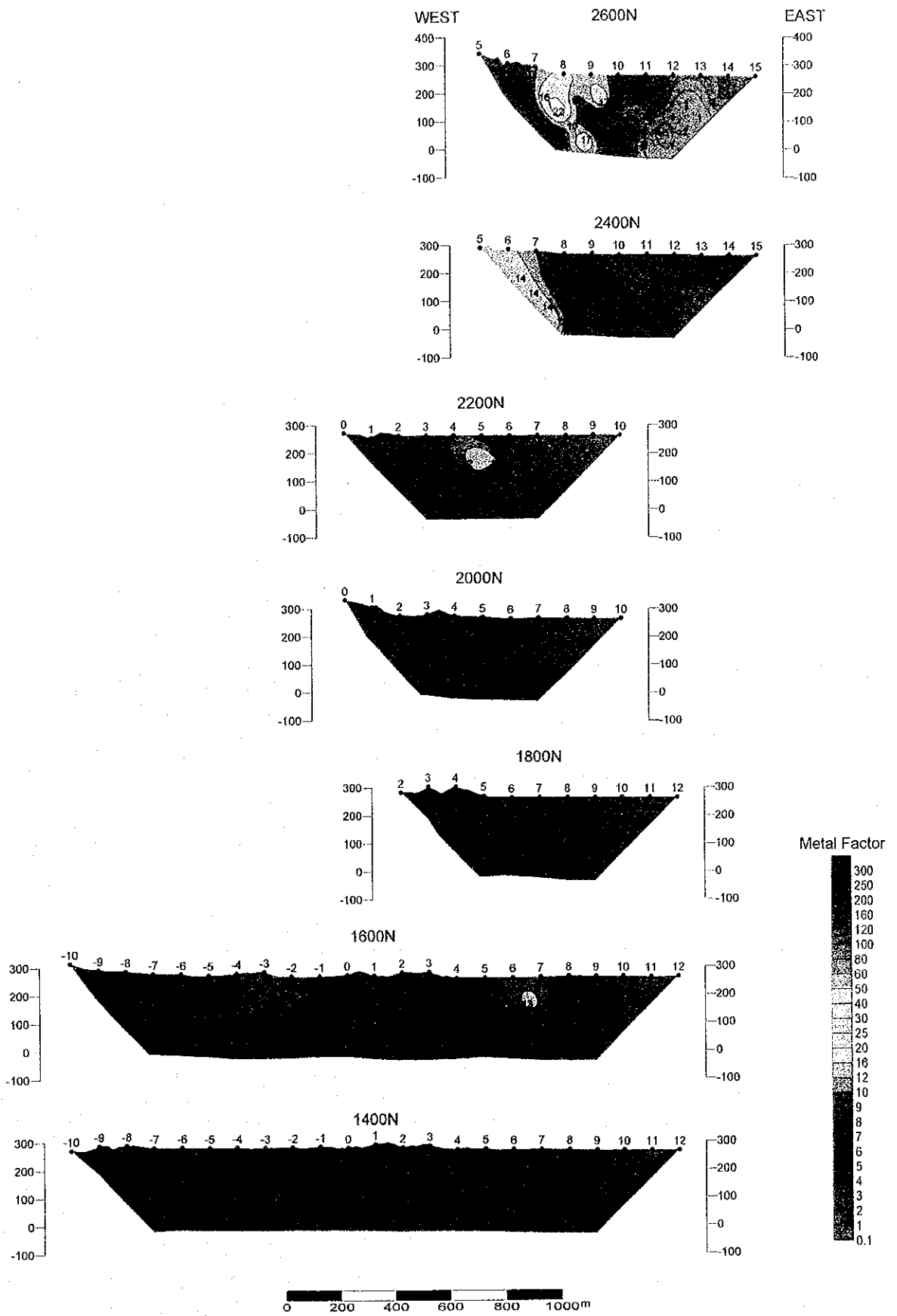


Fig. II -2-41(2) Metal factor pseudo-sections in Salahi area

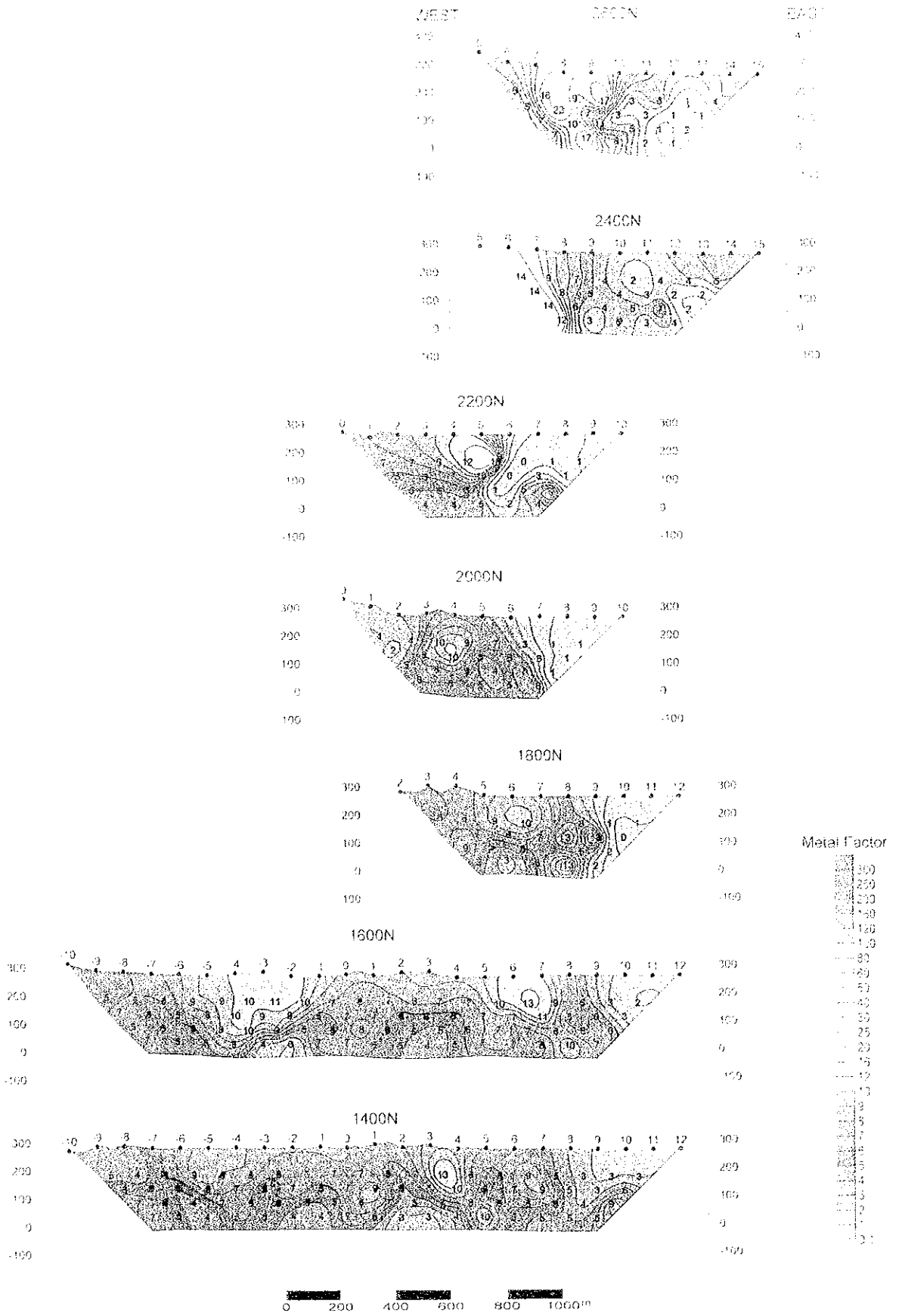
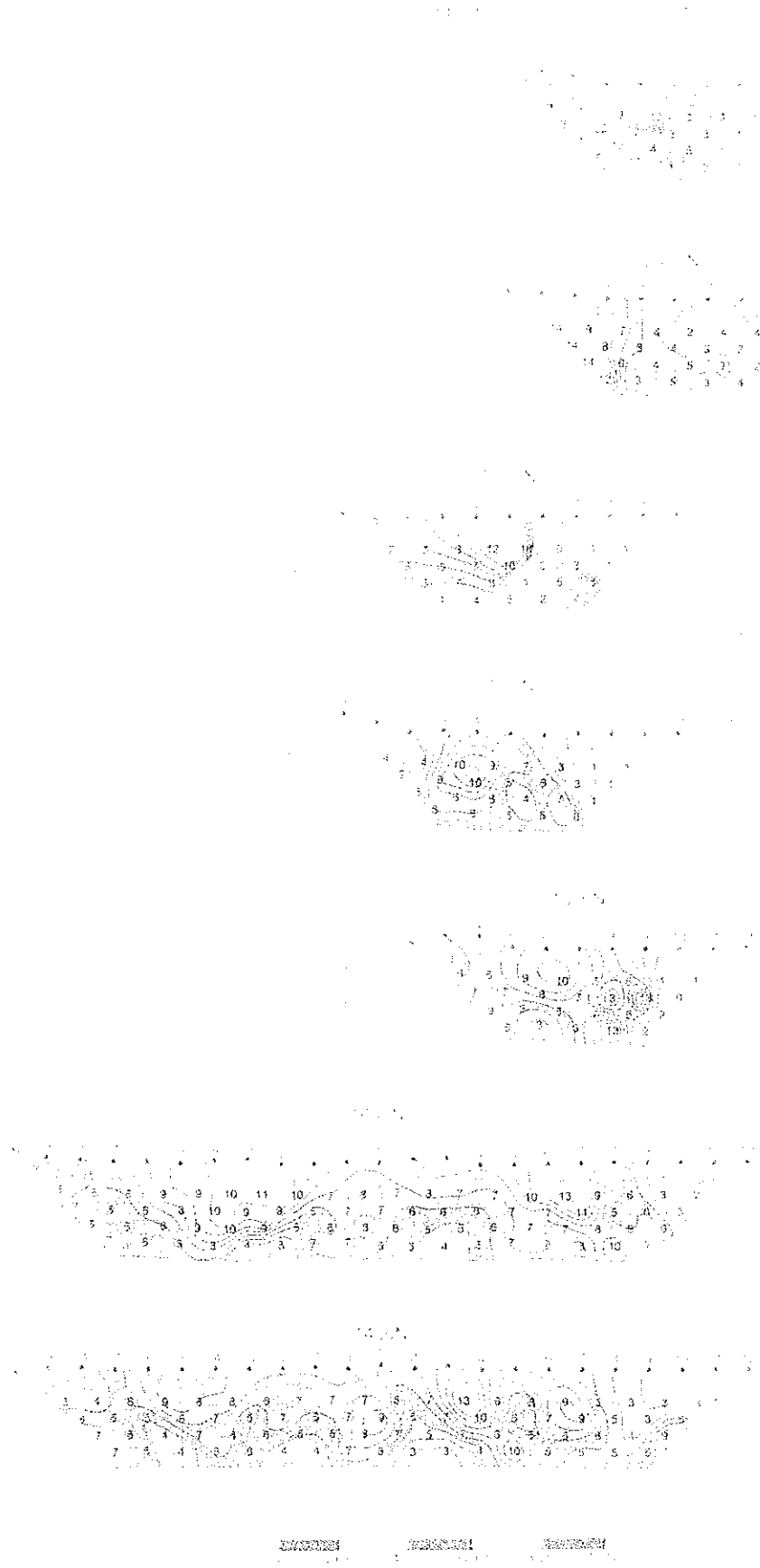
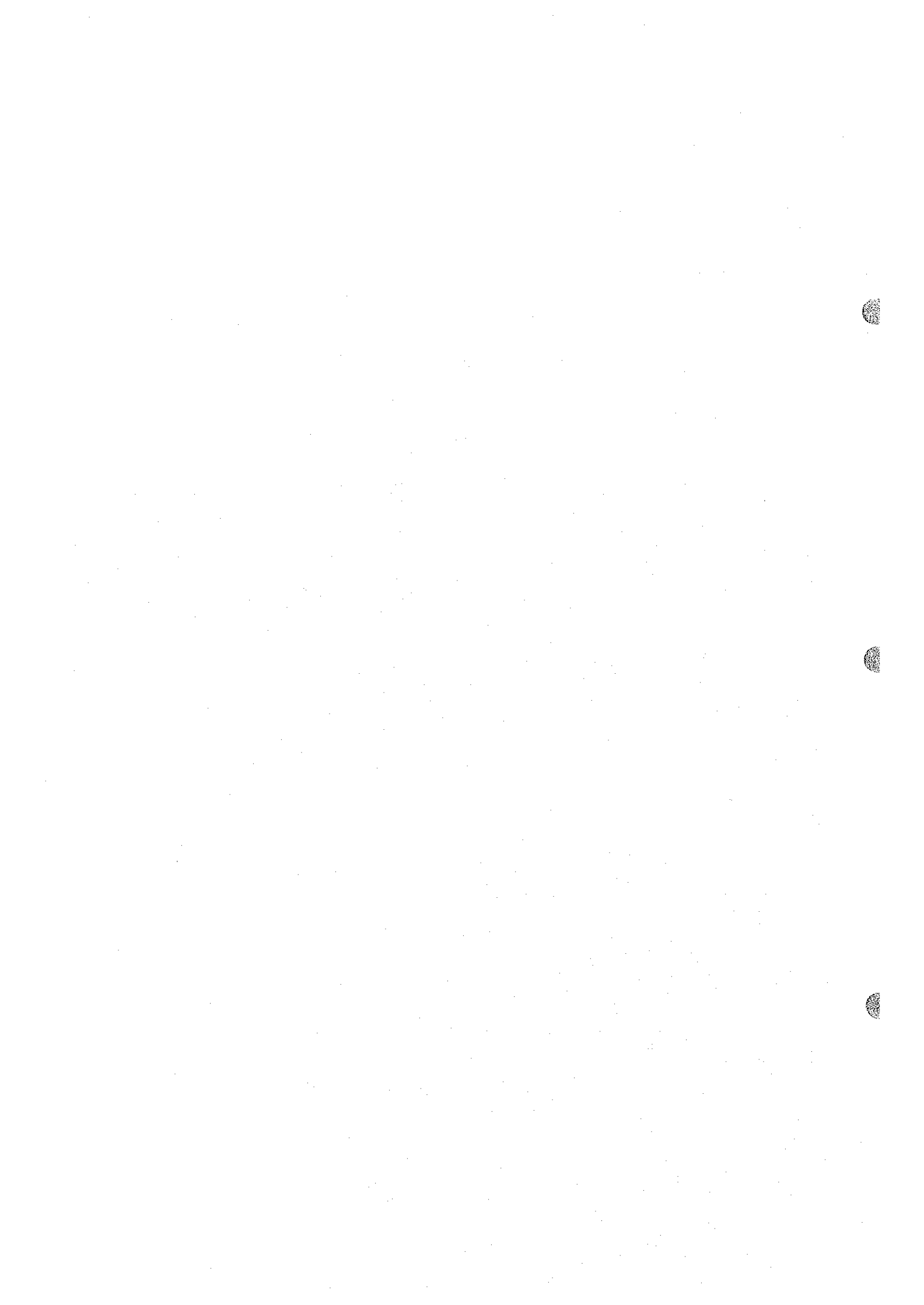


Fig. II-2-41(2) Metal factor pseudo-sections in Salahi area



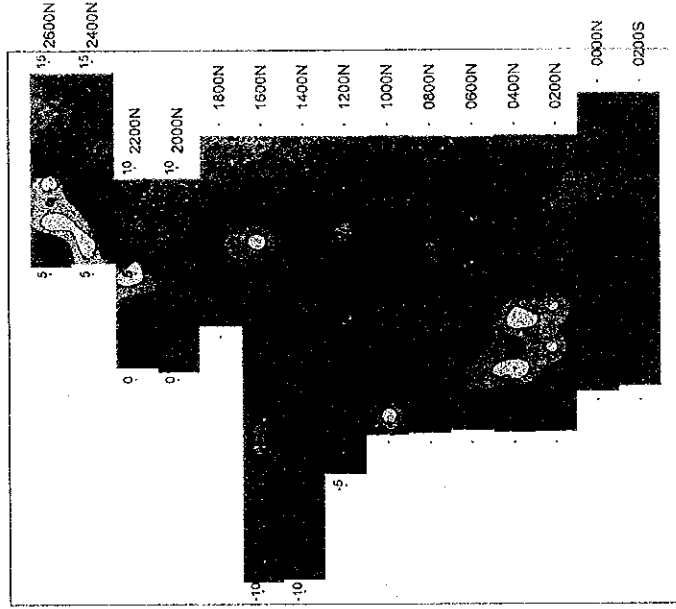
Legend:   
 0-1000   
 1000-2000   
 2000-3000

Fig. 11-2-11-2. Metal distribution in sections of shale unit.

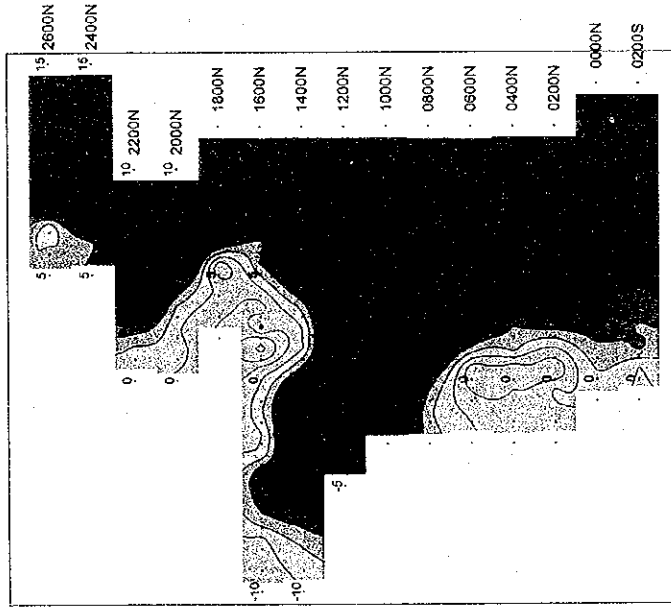




Metal Factor



Chargeability



Apparent Resistivity

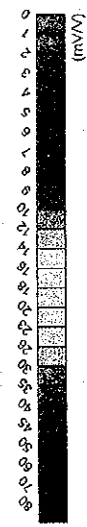
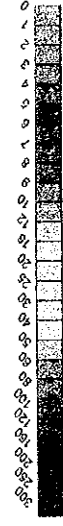
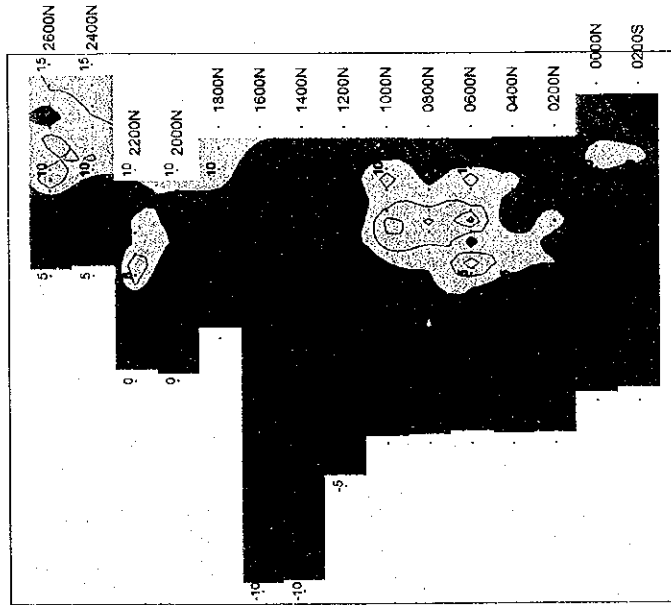
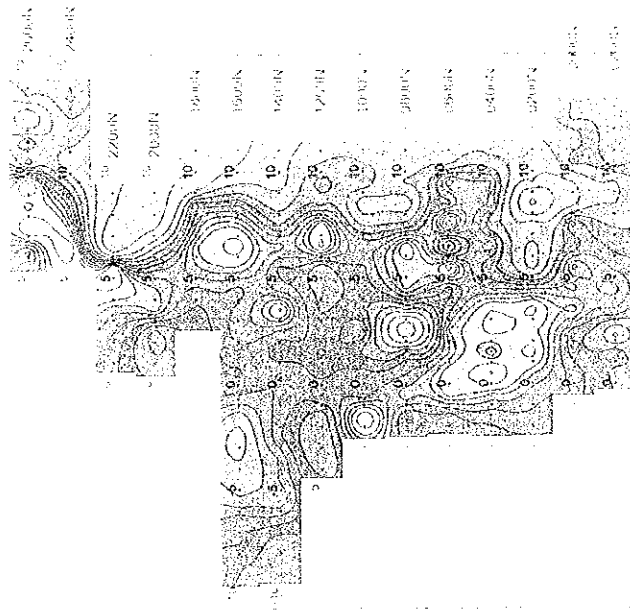


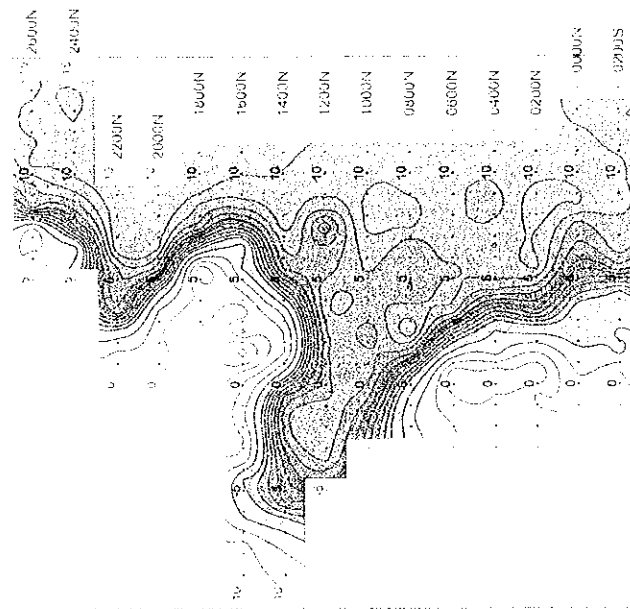
Fig. II -2-42 IP plane map of n=1 in Salahi area

1.

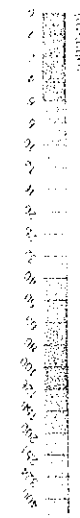
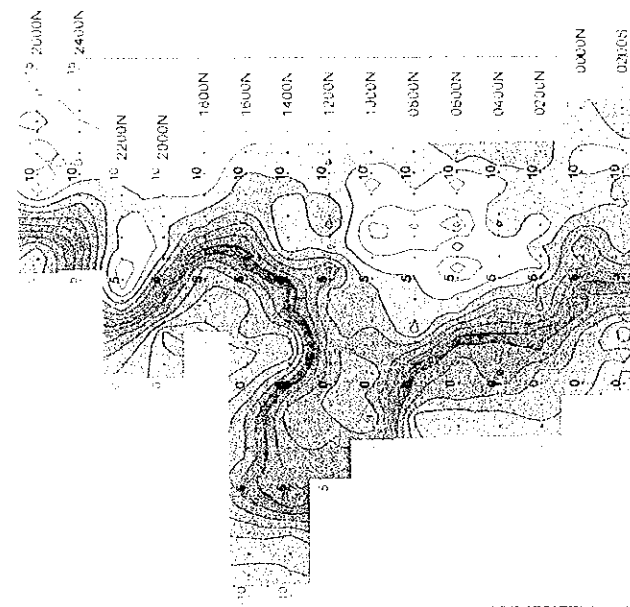
Metal Factor



Chargeability



Apparent Resistivity



0 500 1000 1500 2000<sup>m</sup>

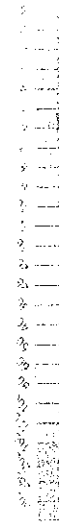


Fig. II-2-42 IP plane map of n=1 in Salahi area



Figure 77

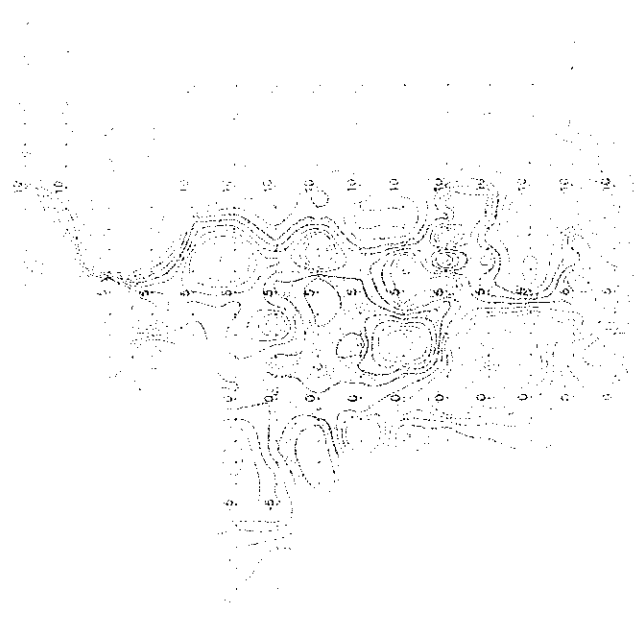


Figure 78

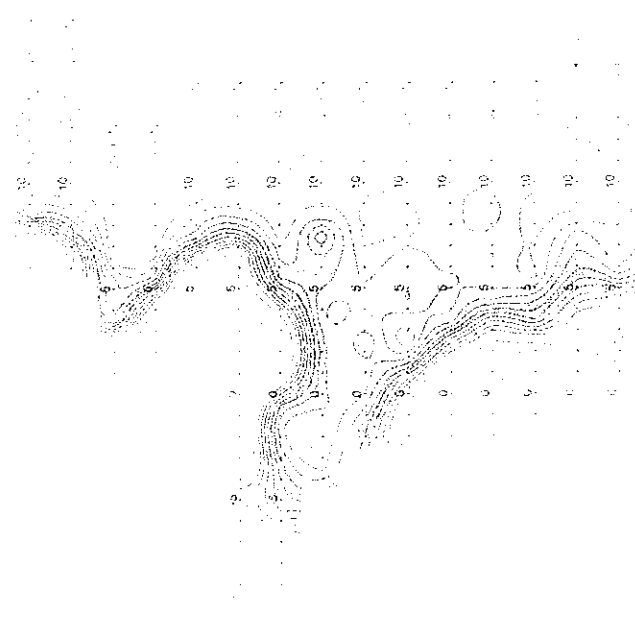
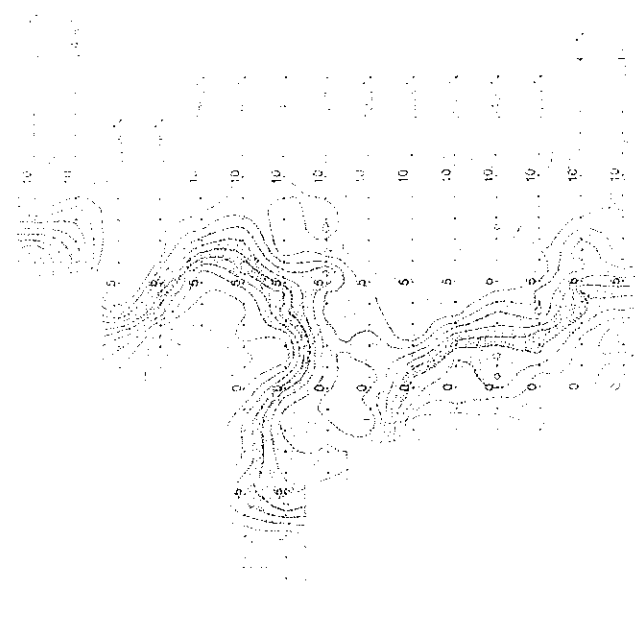


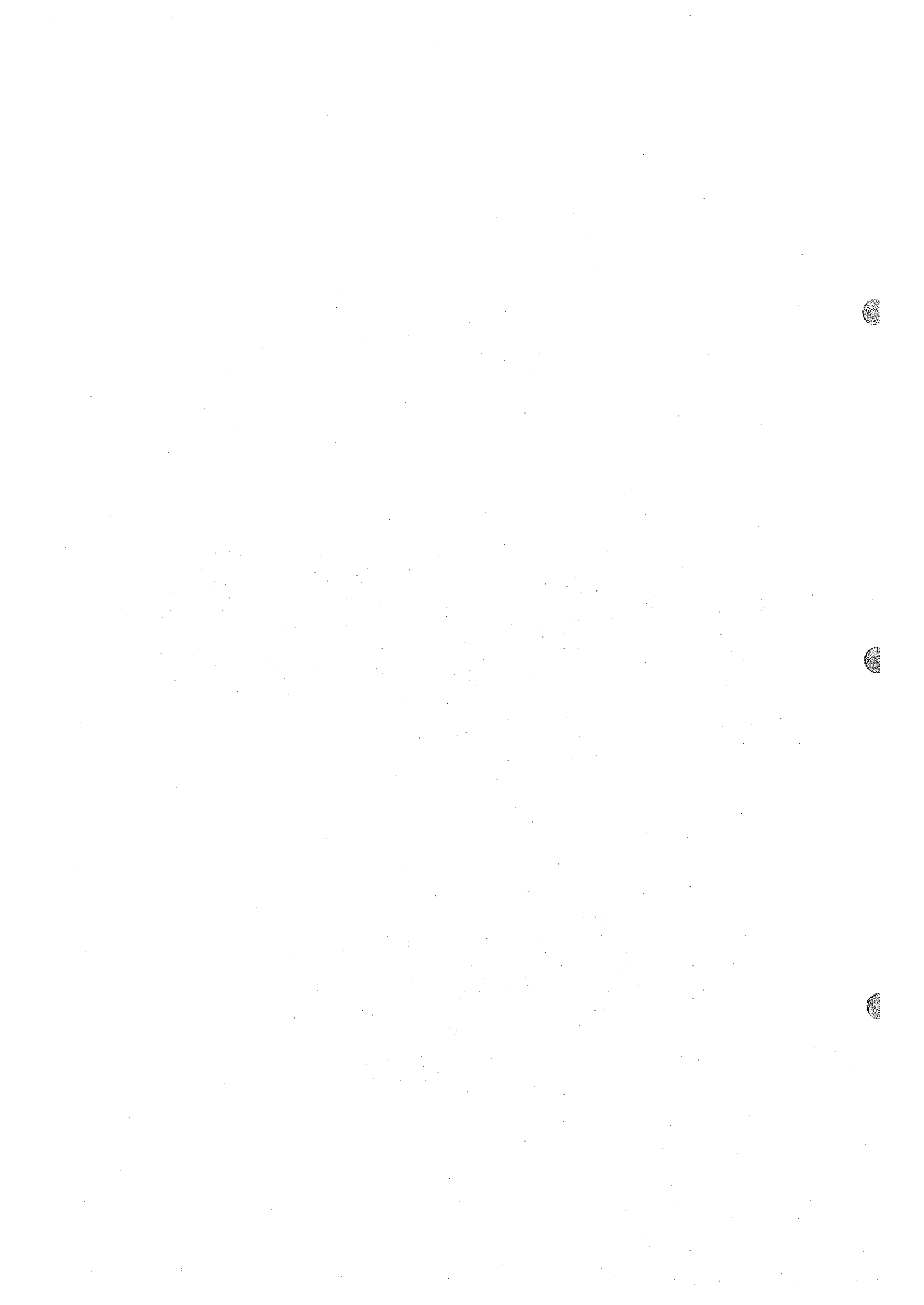
Figure 79



APPARENT RESISTIVITY (OHMS) vs. FREQUENCY (CYCLES PER SECOND)

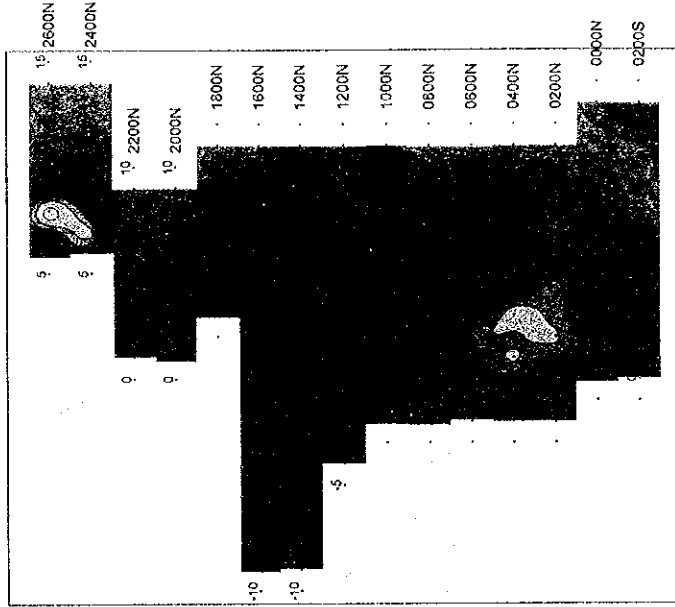
RESISTIVITY (OHMS) vs. FREQUENCY (CYCLES PER SECOND)

RESISTIVITY (OHMS) vs. FREQUENCY (CYCLES PER SECOND)

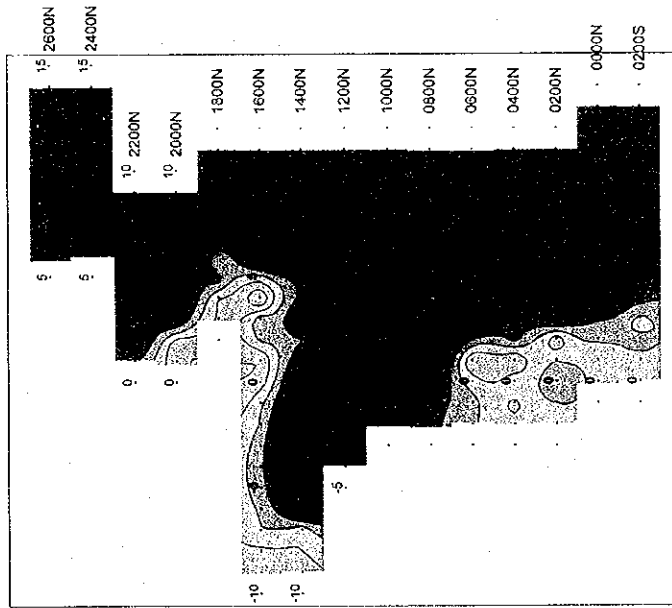




Metal Factor



Chargeability



Apparent Resistivity

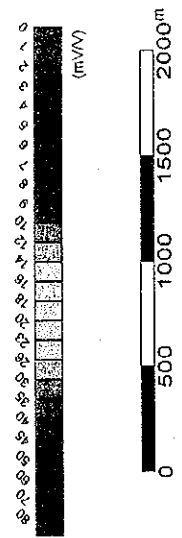
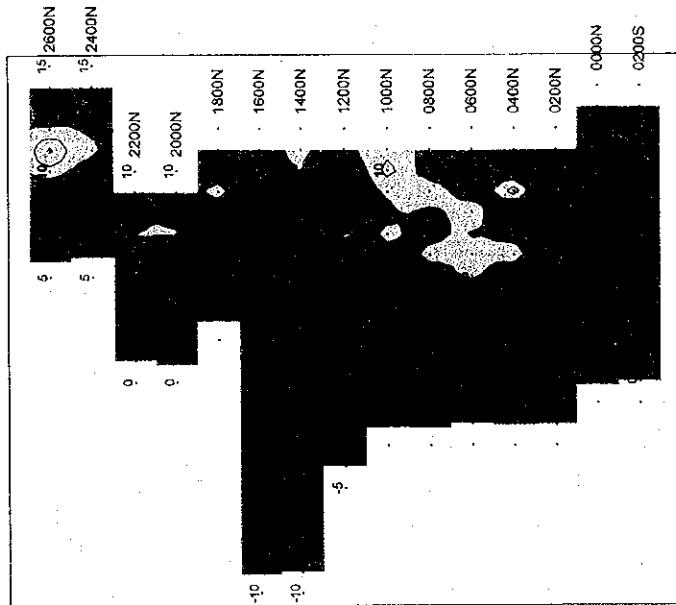


Fig. II -2-43 IP plane map of n=2 in Salahi area

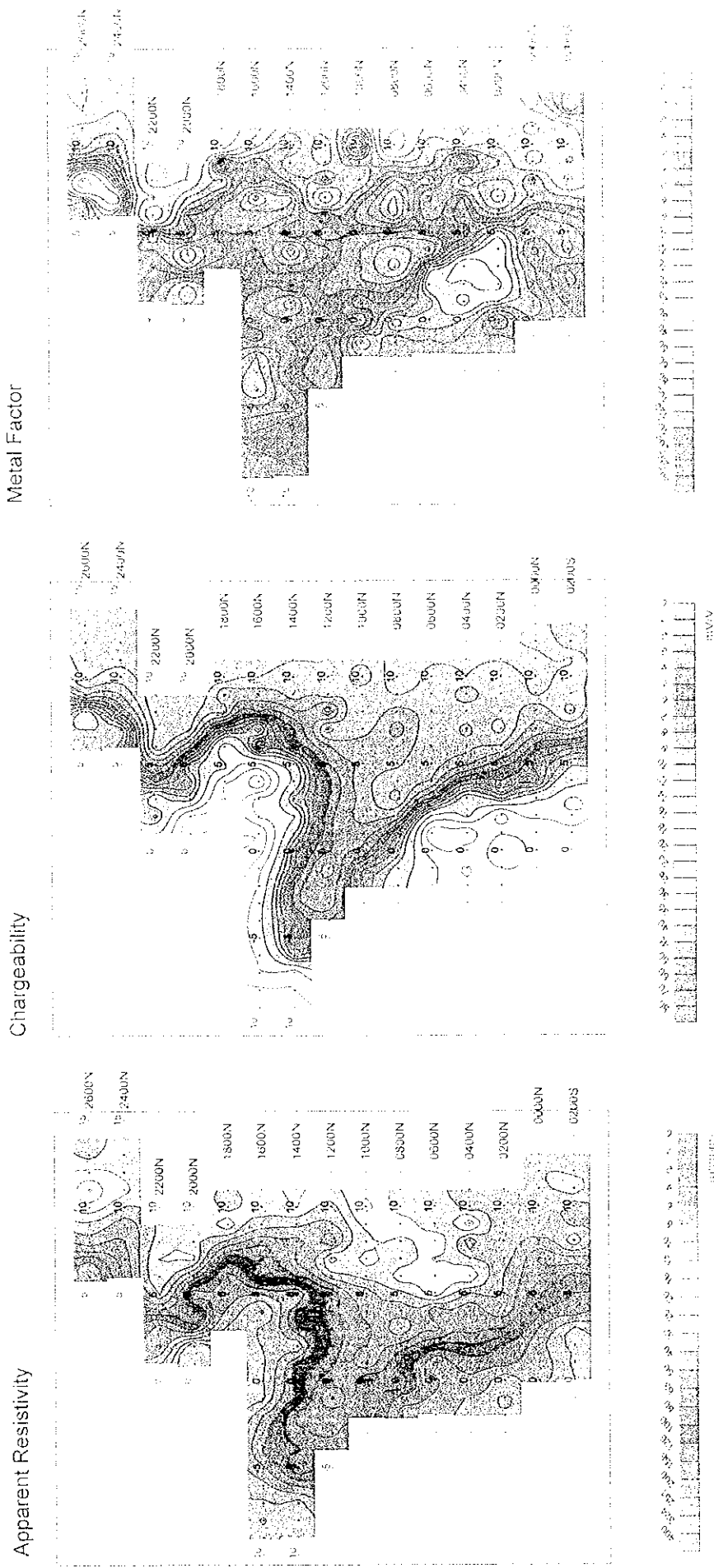


Fig. II -2-43 IP plans map of n-2 in Salahi area

Apparent Resistivity

Chargeability

Depth in m

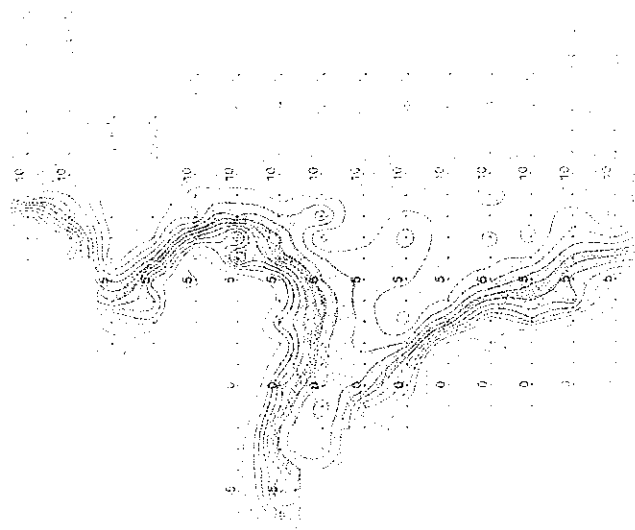
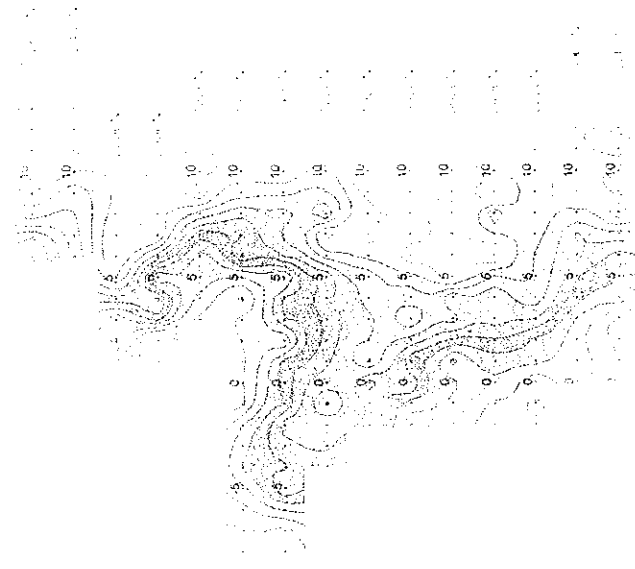
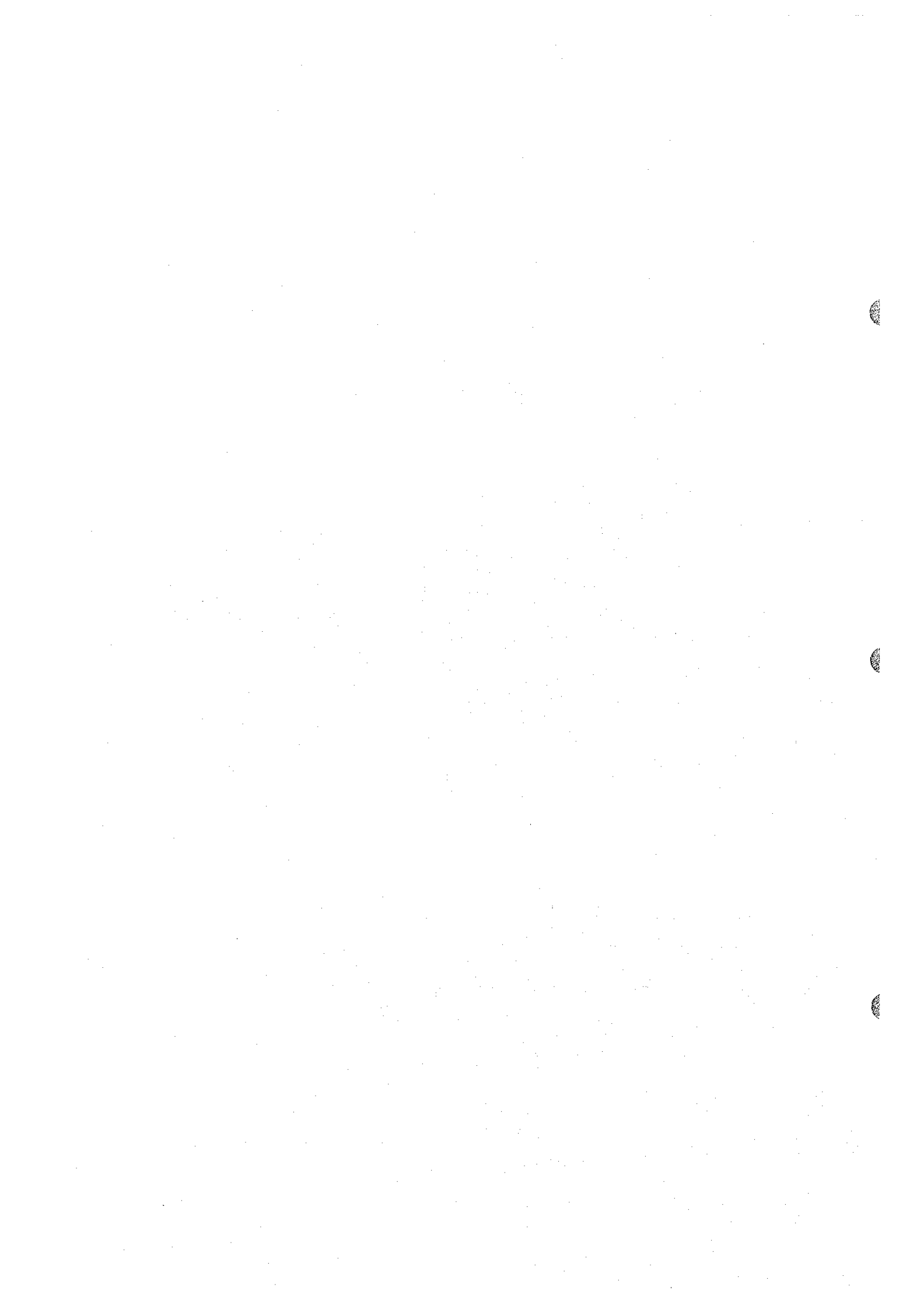


Figure 1. Apparent resistivity, chargeability, and depth contours for the study area. The contours are drawn at 1 m intervals. The resistivity contours are labeled with values from 0 to 10. The chargeability contours are labeled with values from 0 to 10. The depth contours are labeled with values from 0 to 10. The contours are more densely packed in the central area, indicating steeper gradients.

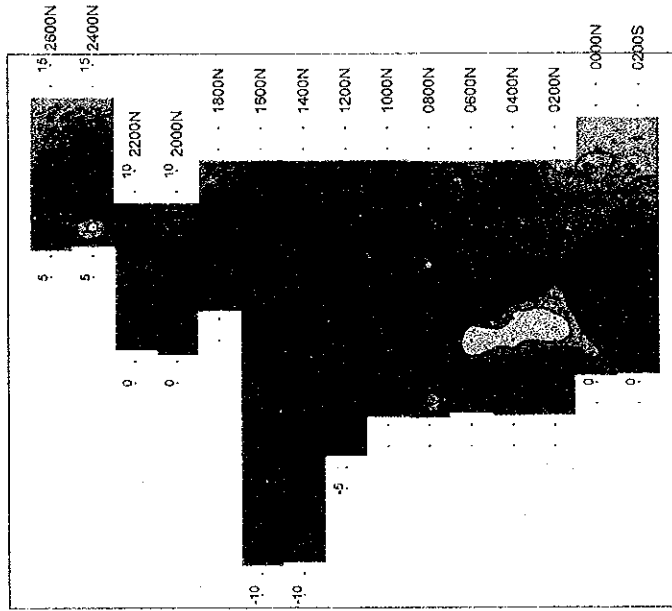
Geological Survey of India, Bangalore

Geological Survey of India, Bangalore

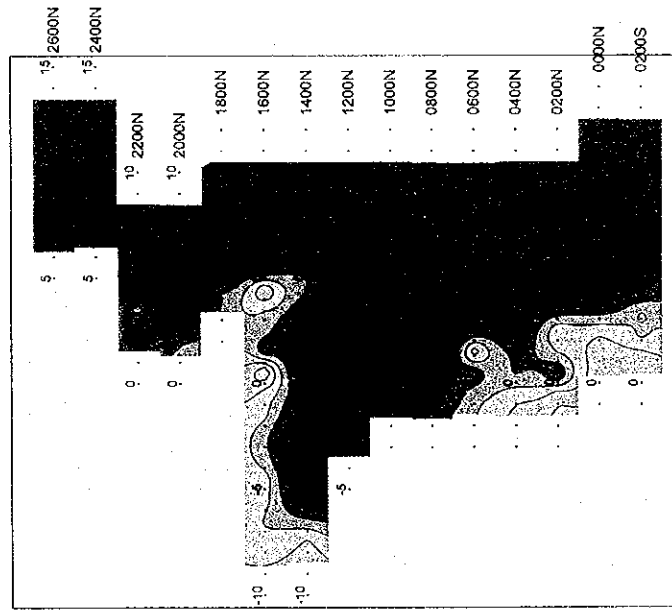




Metal Factor



Chargeability



Apparent Resistivity

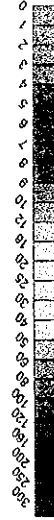
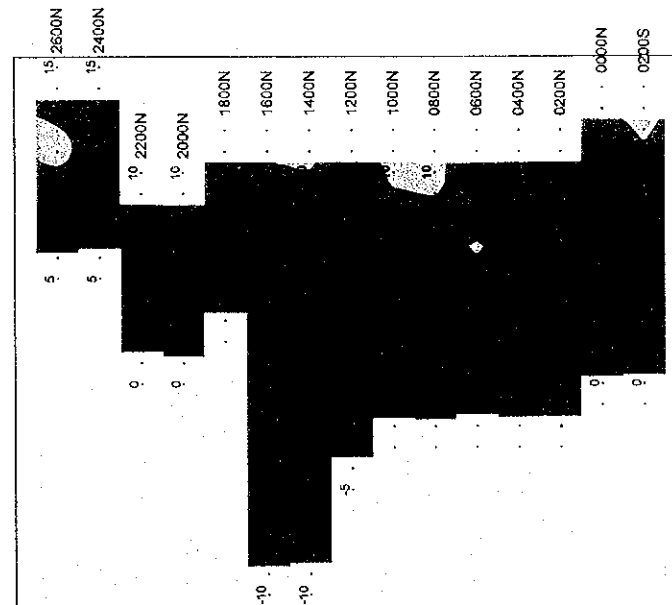
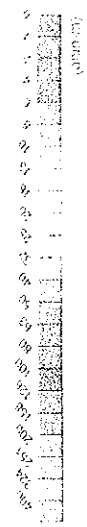
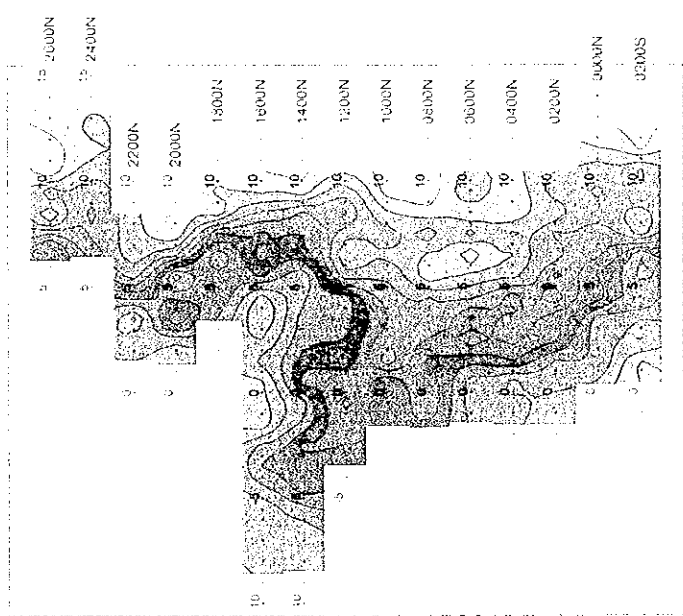
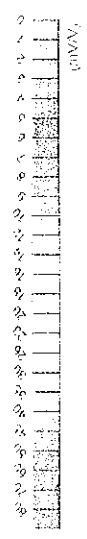
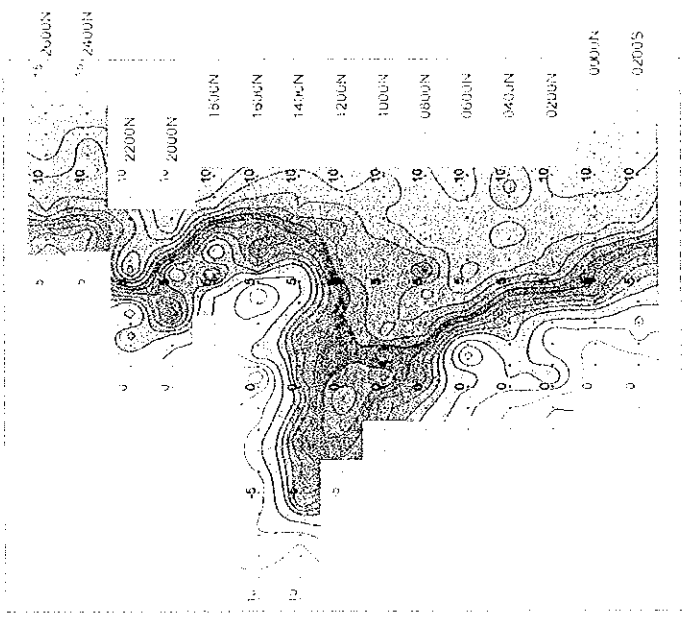


Fig. II -2-44 IP plane map of  $n=3$  in Salahi area

Apparent Resistivity



Chargeability



Metal Factor

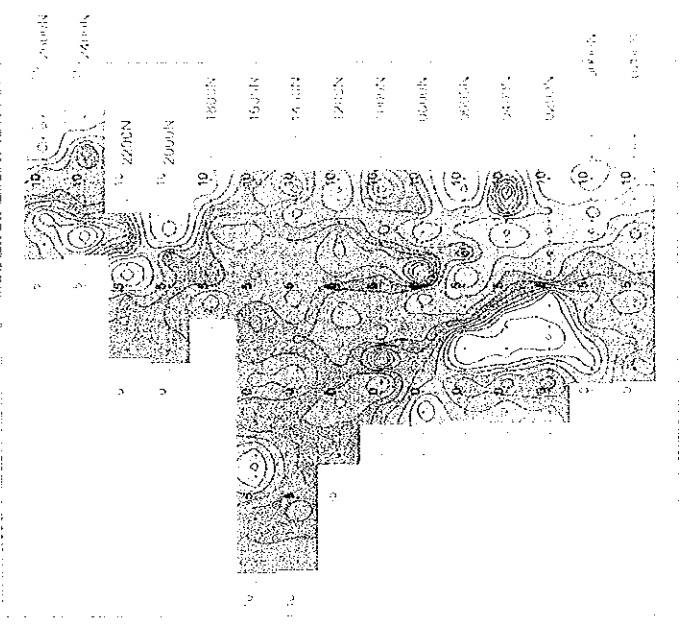
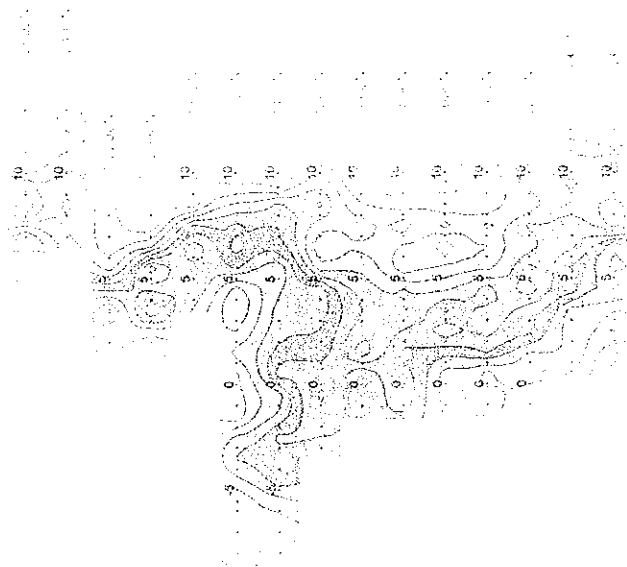


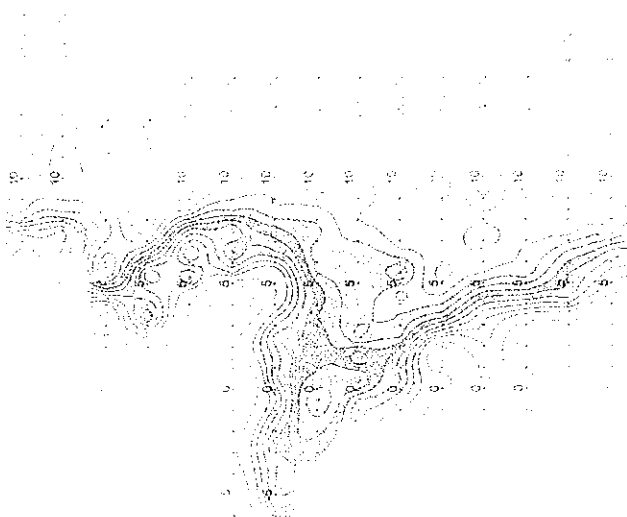
Fig. II -2-44 IP plane map of  $n=3$  in Salahi area



Apparent Resistivity



Chloride by



Moisture by

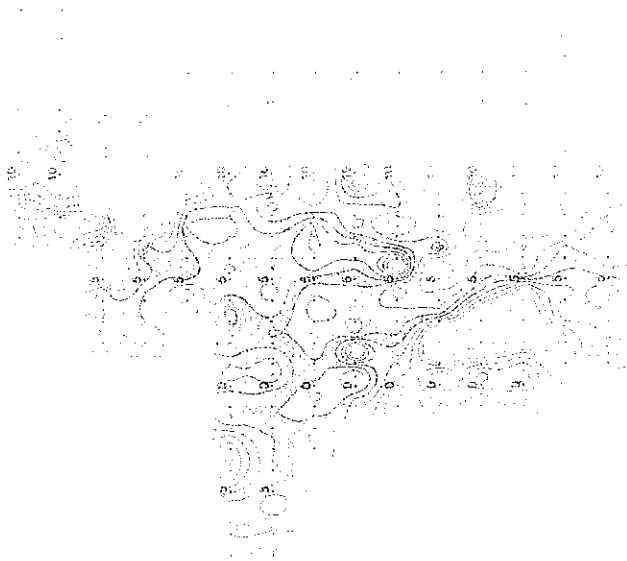
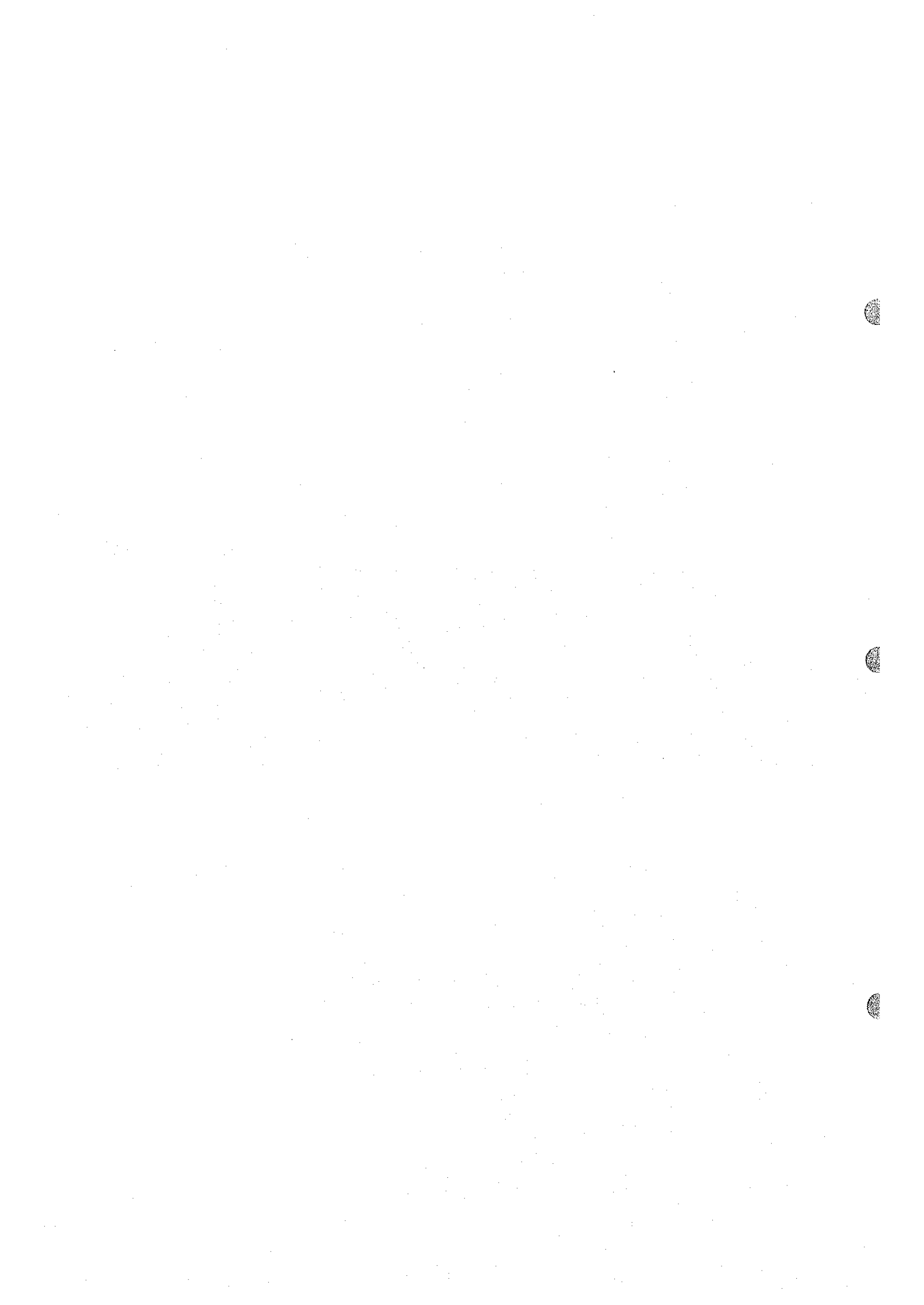


Figure 1. Apparent resistivity, chloride by, and moisture by contours.

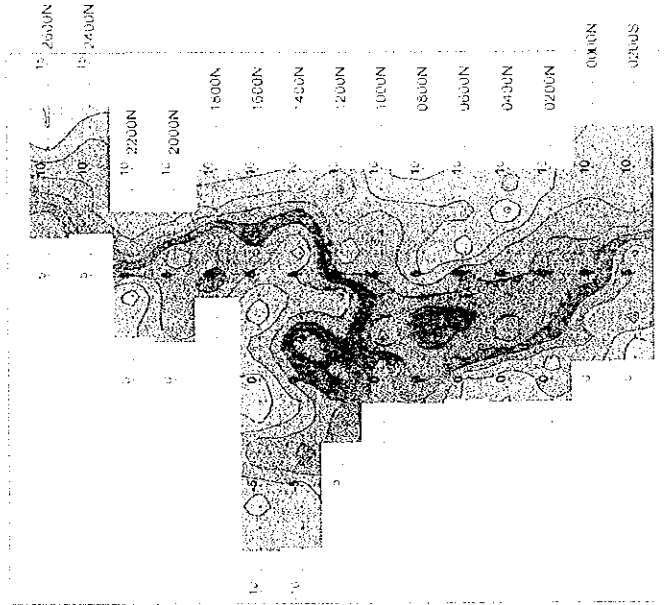
Figure 1. Apparent resistivity, chloride by, and moisture by contours.

Figure 1. Apparent resistivity, chloride by, and moisture by contours.

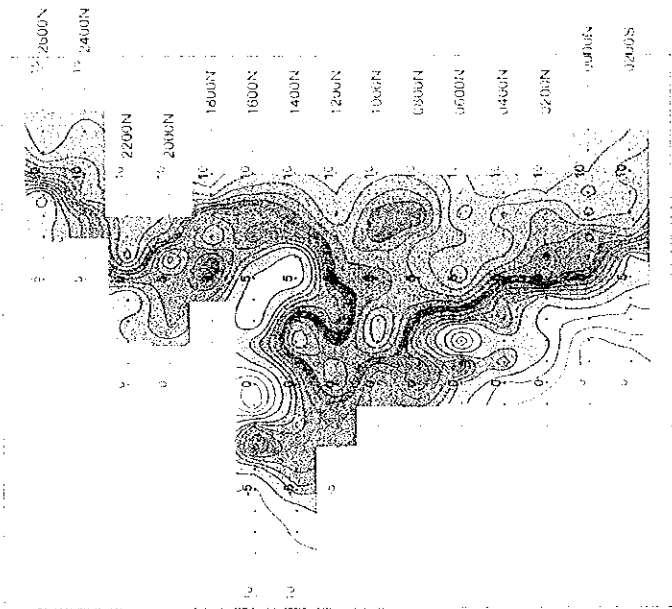




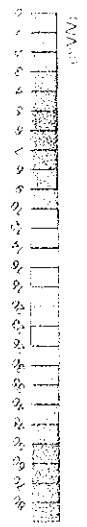
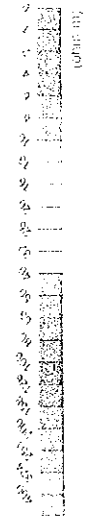
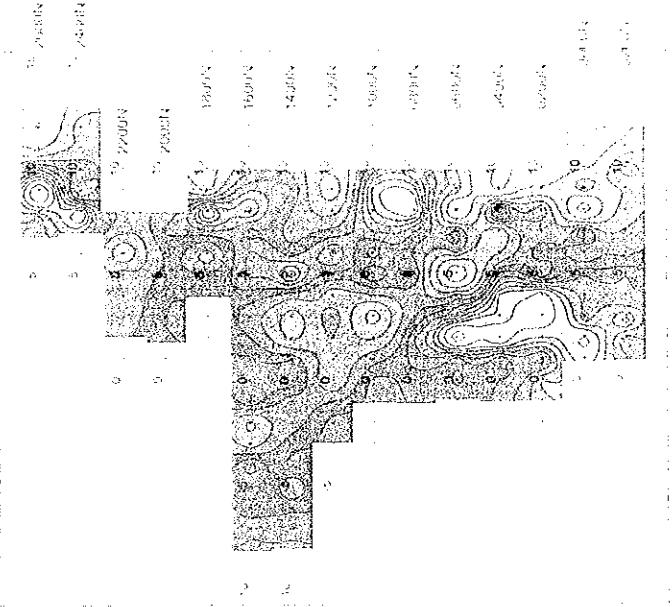
Apparent Resistivity



Chargeability



Metal Factor



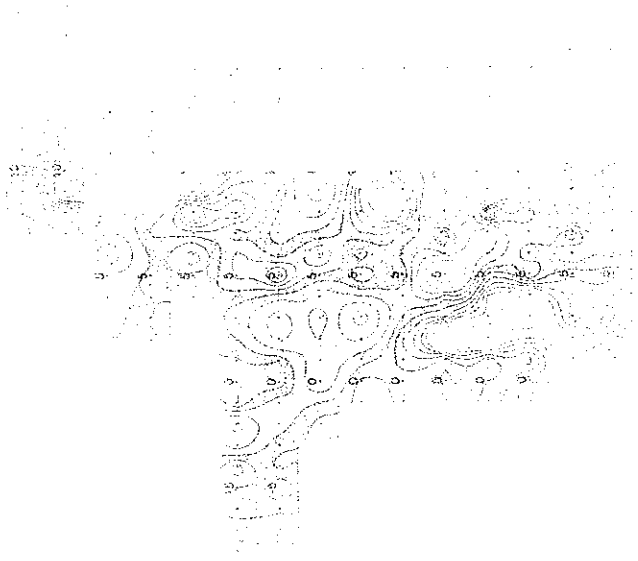
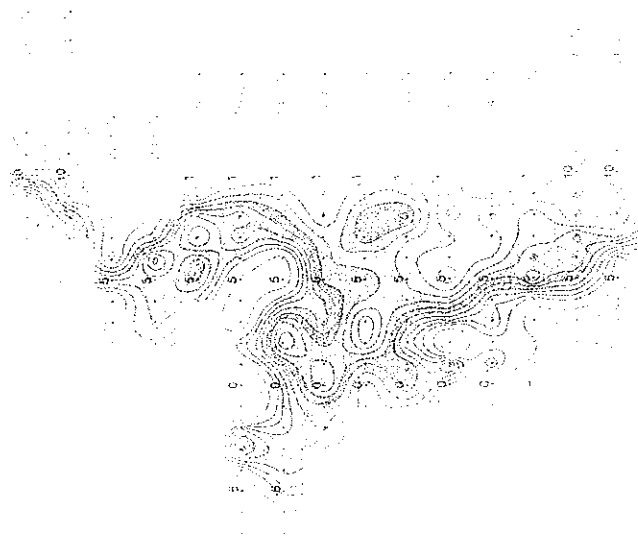
0 500 1000 1500 2000

Fig. U-2-45 IP plane map of n-4 in Salahi area

Apparent Resistivity

Chargeability

Depth of Investigation



10000  
5000  
1000  
500  
100  
50  
10  
5  
1

10000  
5000  
1000  
500  
100  
50  
10  
5  
1

10000  
5000  
1000  
500  
100  
50  
10  
5  
1

10000  
5000  
1000  
500  
100  
50  
10  
5  
1

10000  
5000  
1000  
500  
100  
50  
10  
5  
1



station No.7 and between the lines 600N to 1000N at shallow levels, low resistivity anomaly of values less than  $20 \Omega \cdot m$  can be recognized. However, this anomaly distribution presents chargeability values lower than  $5mV/V$ . On the other hand, between the lines 200N to 600N and in the surroundings of the station No.2, relatively high metal factor values are detected which may correspond geologically to the V1-I formation, for which this anomaly can not be related to any massive sulphide mineralization.

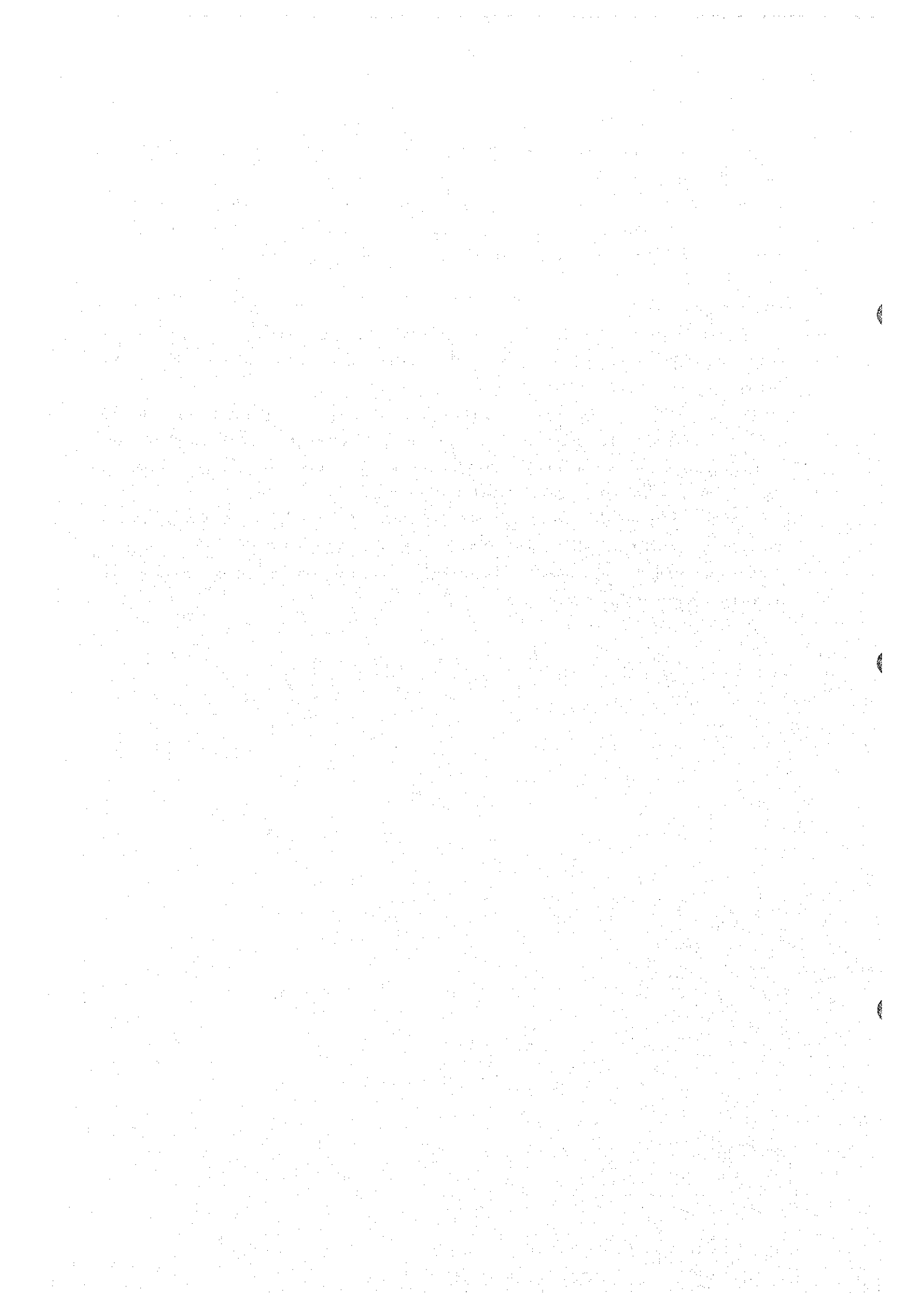
### **(3) 2D analysis**

2D analysis was performed for all the lines, but here for matter of convenience, only the sections containing representative anomalies will be described. On these regards, only the 2D results of lines 200N and 600N will be briefly described (Fig. II -2-46).

In relation to the line 200N, low to medium resistivity values are seen at shallow levels below the stations Nos.5 to 8. High chargeability values with a maximum of  $20mV/V$  are seen around the station No.0 at depths of about 150m. Metal factors comparatively high are seen between the stations Nos.0 and 1 at depth of about 120m and also at superficial levels around station No.4.

In relation to the line 600N, high chargeability zone of more than  $20mV/V$  is detected at the depth of station No.0, however, this zone shows high resistivity values of more than  $150 \Omega \cdot m$

In consequence, these results indicate that there is not any possibility to find any promising zone related to the existence of massive sulphide.





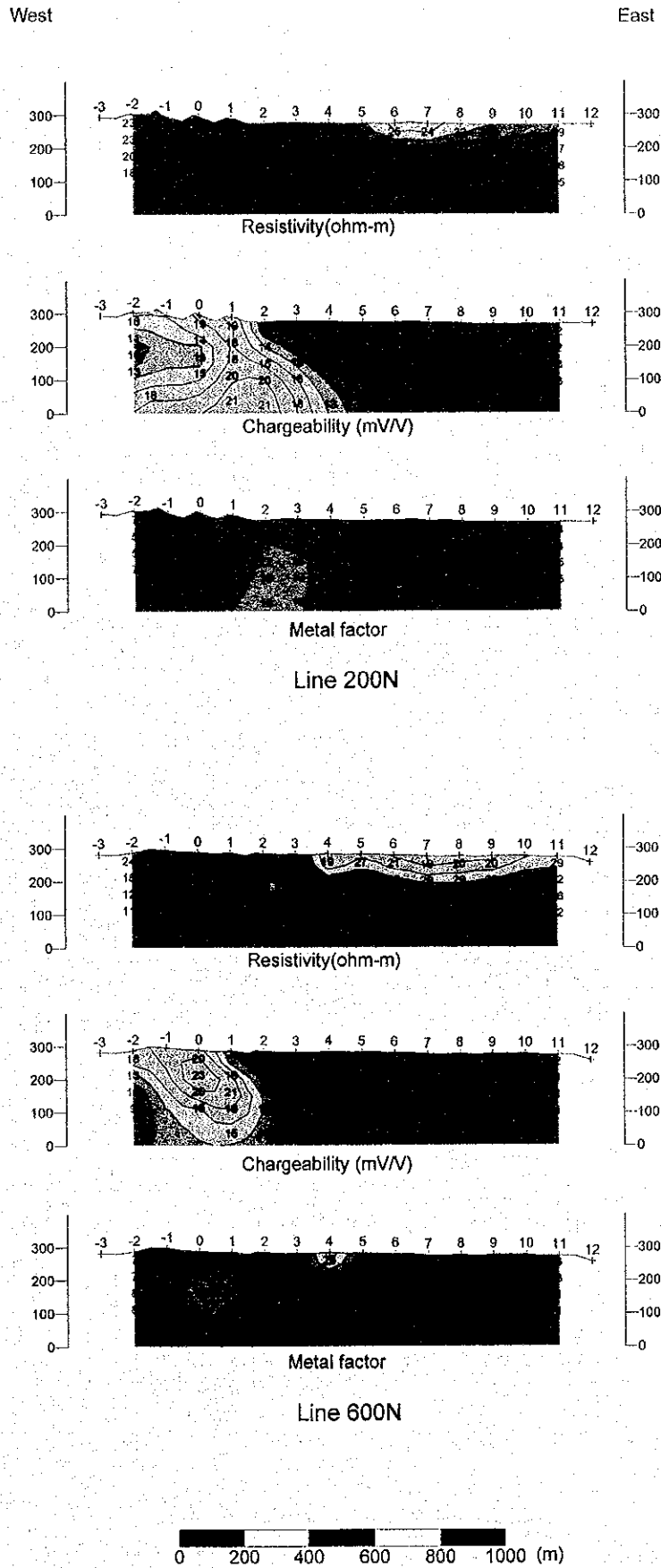


Fig. II -2-46 IP 2D model simulation on lines 200N and 600N in Salah area

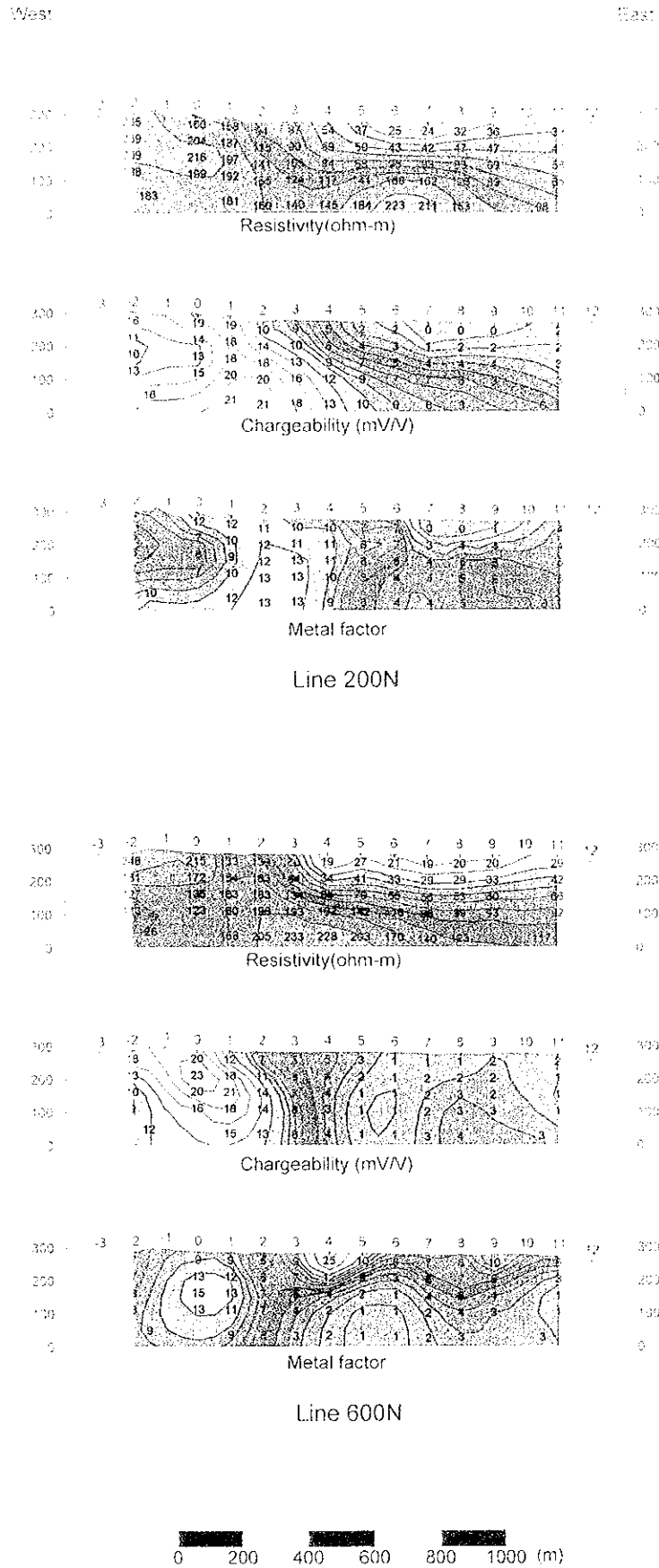


Fig. II -2-46 IP 2D model simulation on lines 200N and 600N in Salahi area

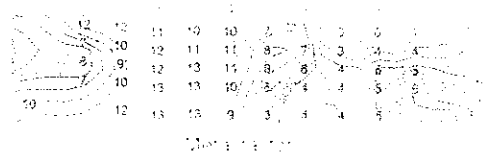
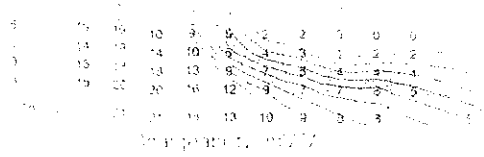
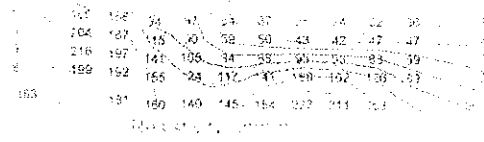


Figure 1-3

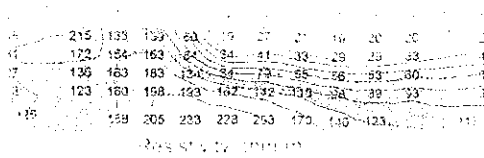


Figure 4

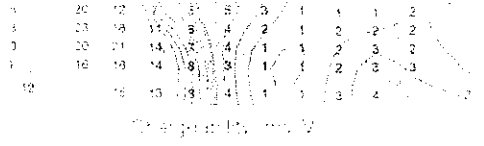


Figure 5

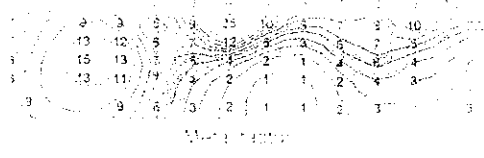
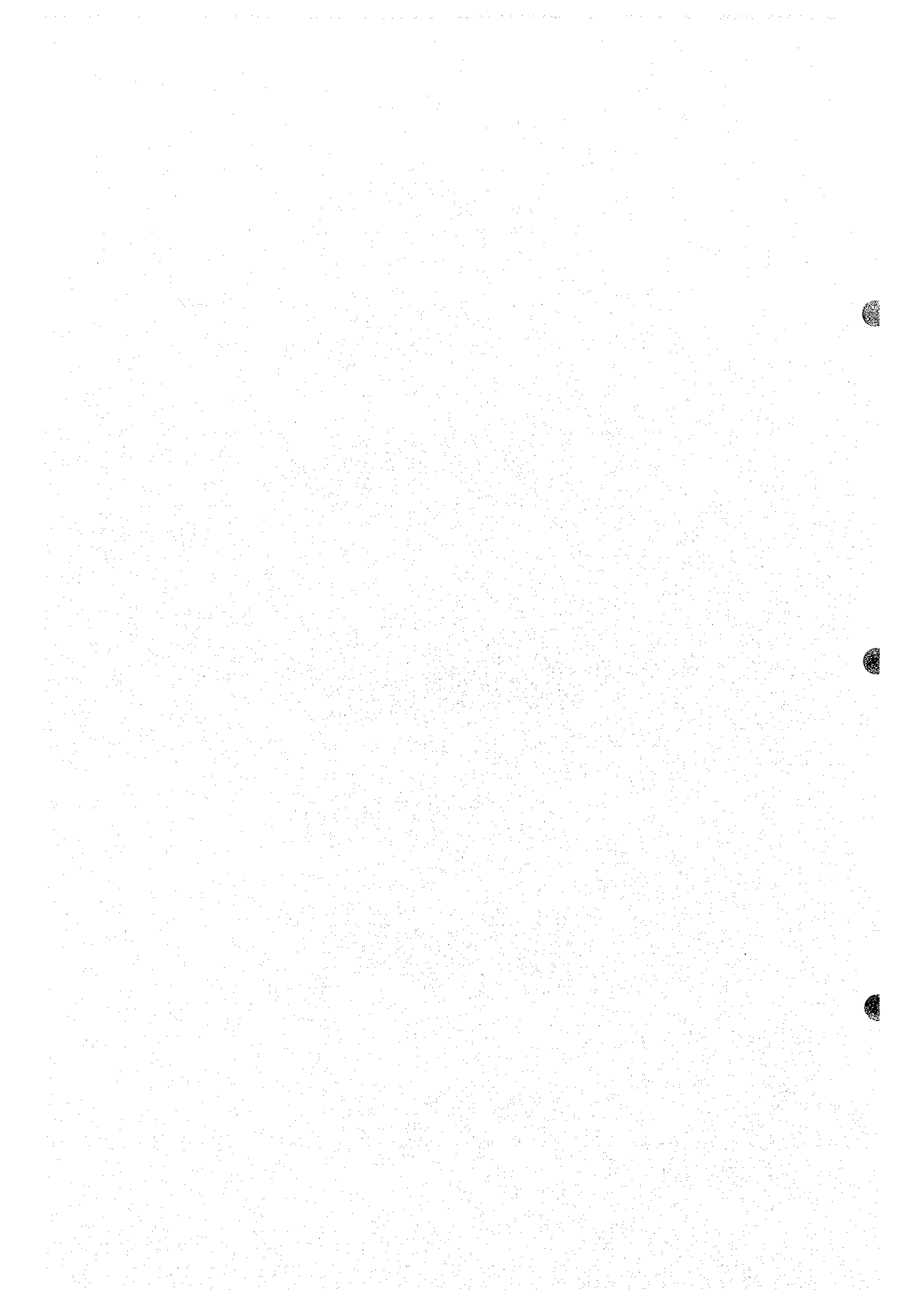


Figure 6

Figure 1-6

Figure 1-2-18: 100 iterations of the gradient method for the function  $f(x, y) = 2x^2 + 2y^2 - 4x - 4y$ .



## **2-6 Further Considerations**

Further considerations regarding Ghuzayn east and west side, Salahi area as well as Zuha area are also presented in Chapter 3 (Section 3-6)

### **2-6-1 Ghuzayn area**

Fig. II-2-47 shows the compiled geophysical map of the surveys carried in Ghuzayn during this year.

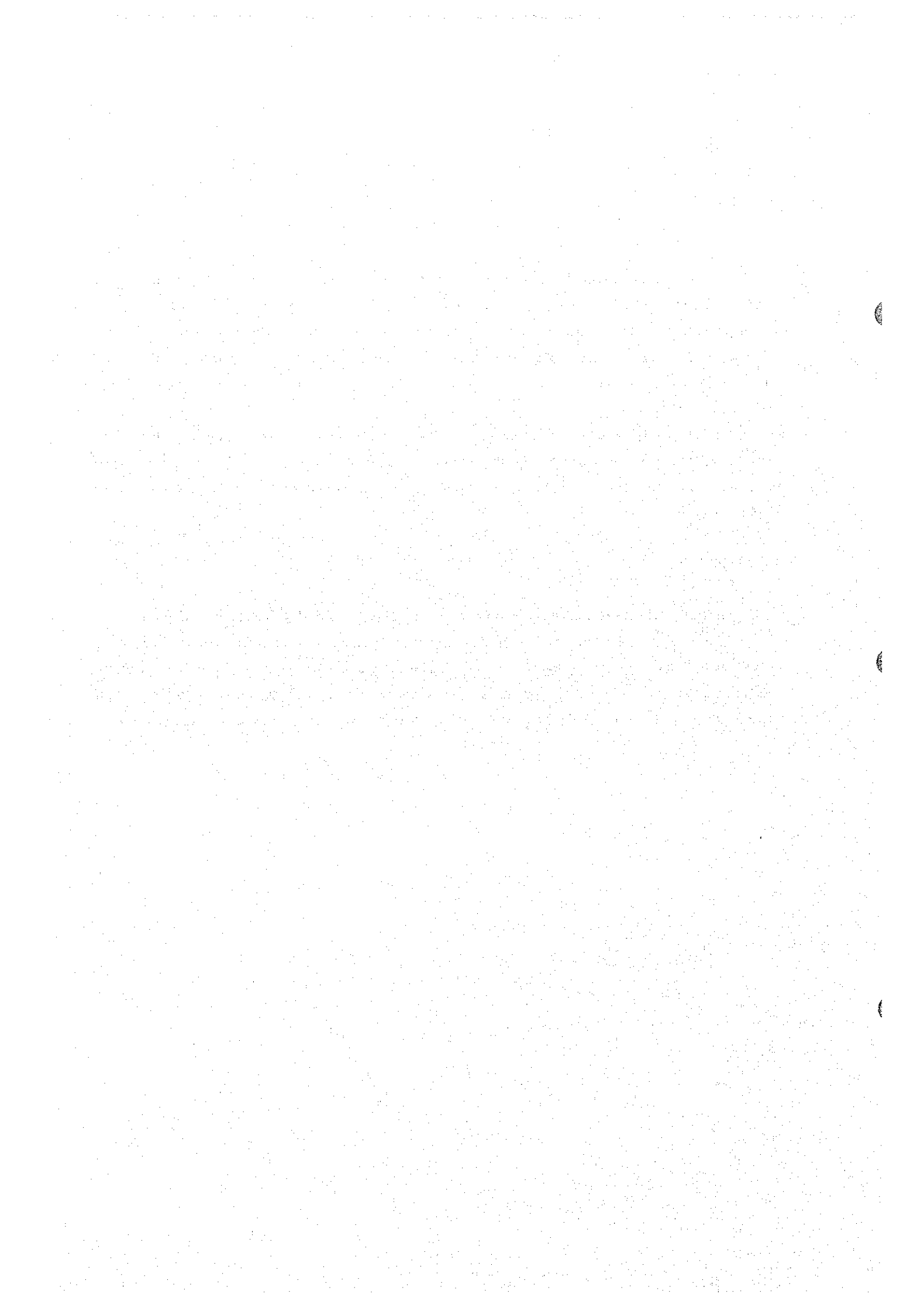
In the east part of Ghuzayn area, in the south part of the lines 1600E to 2000E surveyed this year, it was obtained a chargeability anomaly of above 8mV/V. However, this distribution did not confirm any suitable metal factor distribution that could lead to a promising mineralization. The above mentioned chargeability distribution, which corresponds to VI-1, presents very low possibilities for the existence of massive sulphide deposits.

In the west part of Ghuzayn, within the lines 600W to 2000W surveyed this year, the south part of the lines 1800W to 2000W indicated some chargeability values of more than 8mV/V. However for the same reason mentioned for the east side, this zone does not present any possibility for the existence of massive sulphide deposits.

### **2-6-2 Salahi area**

Fig. II-2-48 shows the compiled geophysical map of the surveys carried in Salahi area during this year.

In the west part of this surveyed area, relatively wide distributions with chargeability values above 8mV/V were found. However, metal factor anomalous distributions corresponding to these chargeability anomalies were not confirmed. In conclusion, the above mentioned chargeability distribution, which corresponds to VI-1, presents very low possibilities for the existence of massive sulphide deposits.



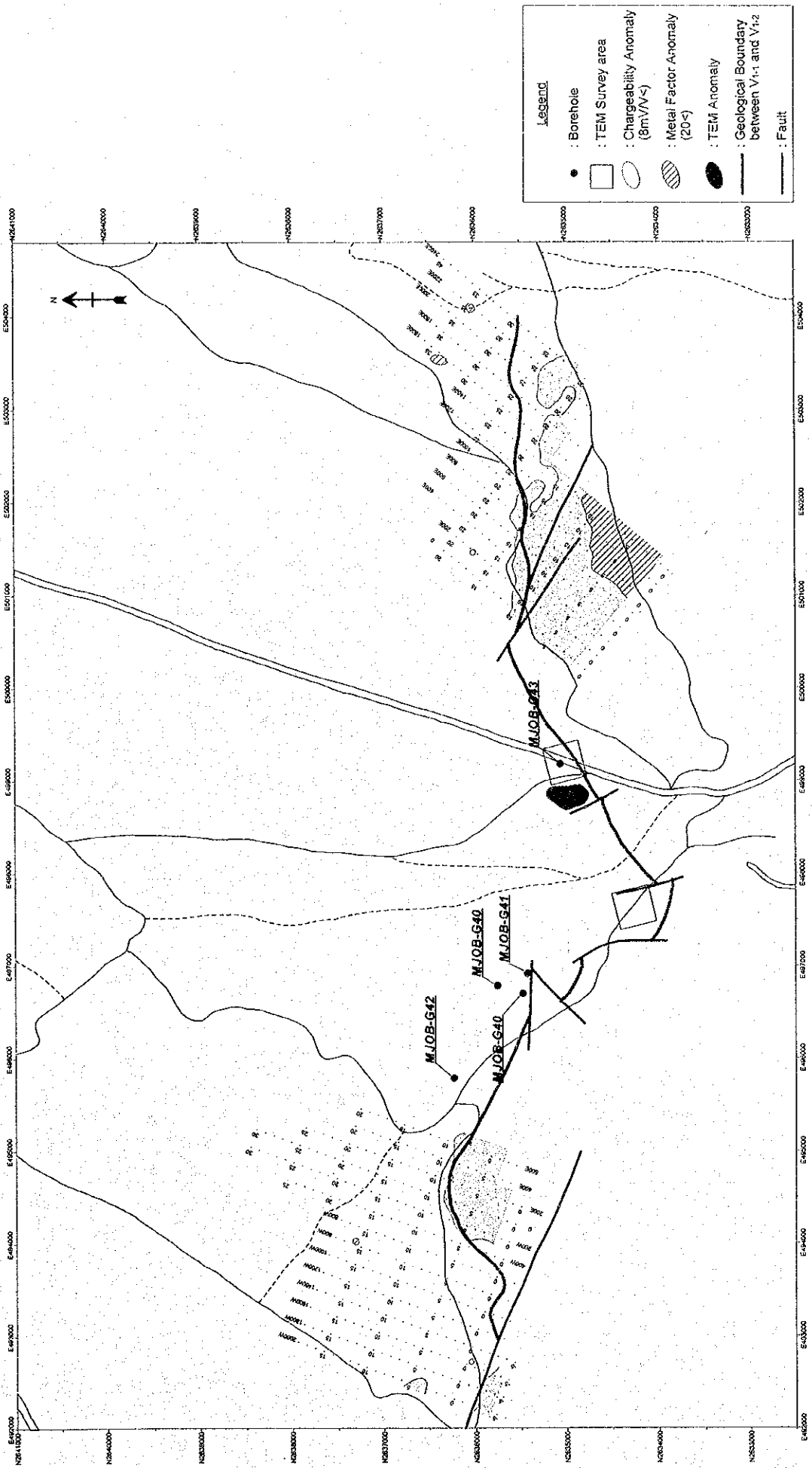
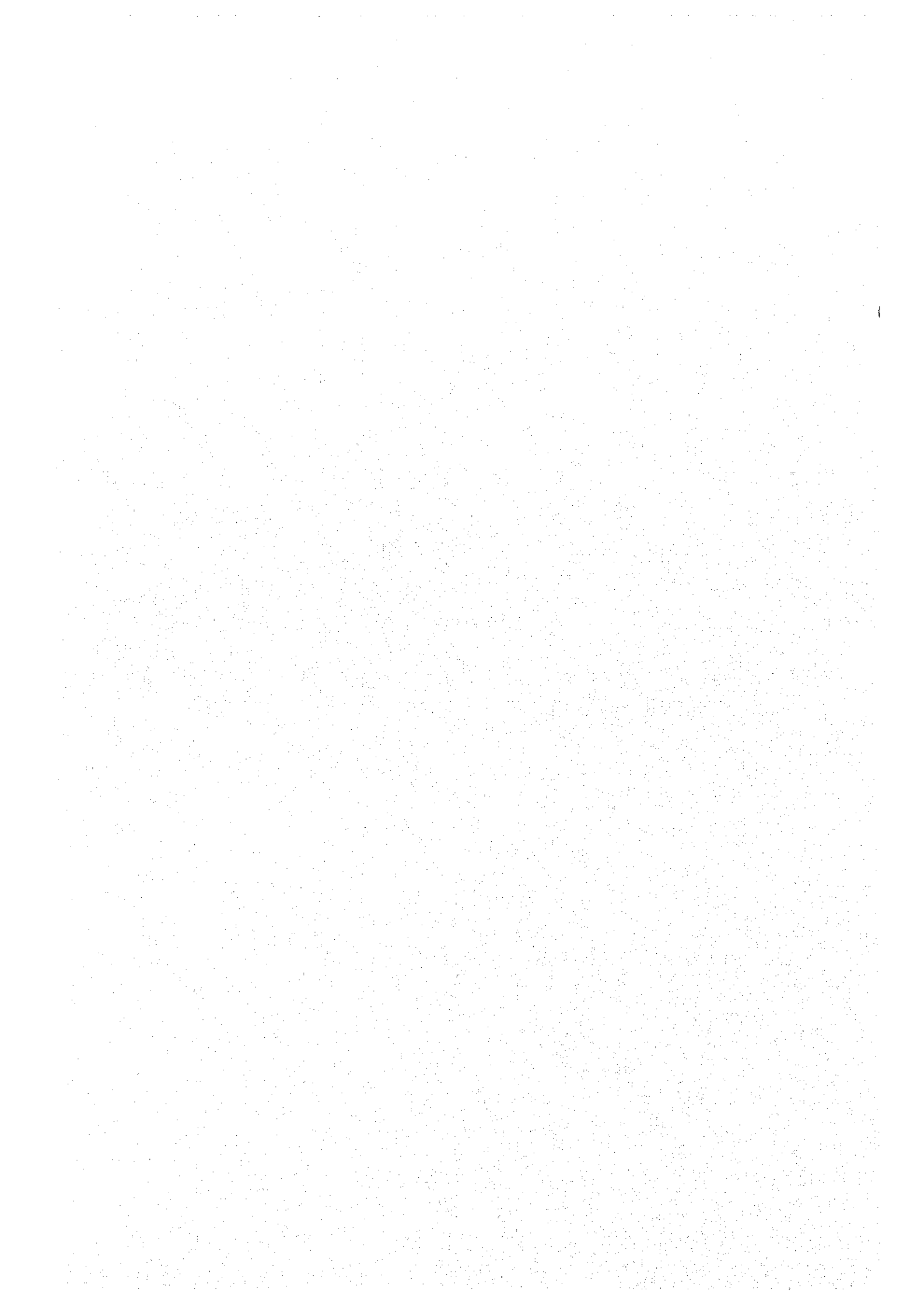


Fig II -2-47 Compiled geophysical map in Ghuzayn area





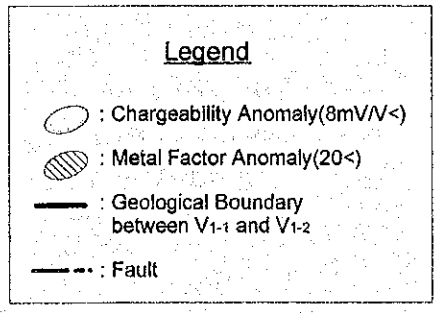
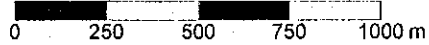
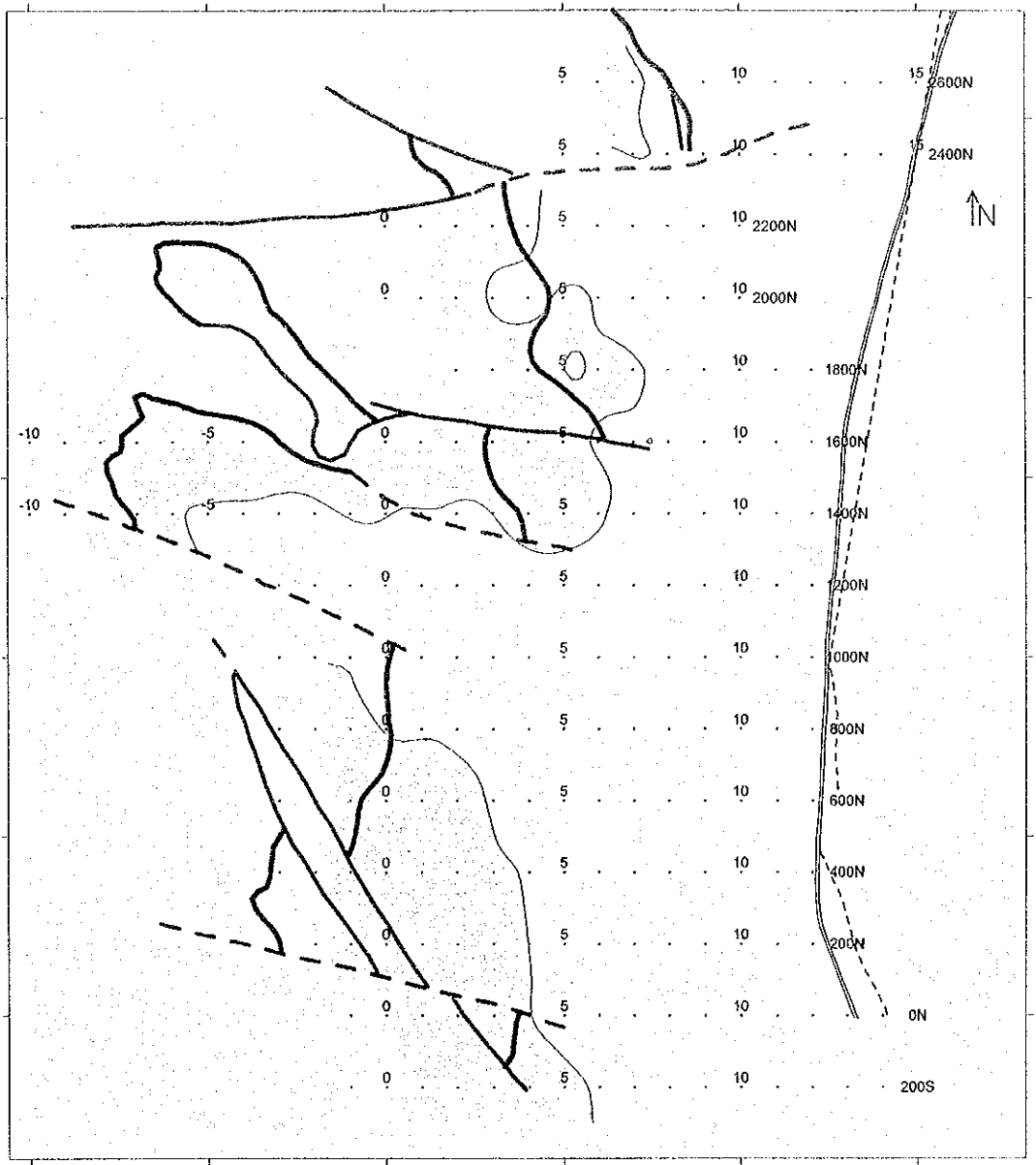


Fig. II -2-48 Compiled geophysical map in Salahi area

